DISCLAIMER

This report was prepared as an account of work sponsored by an agency of the United States Government. Neither the United States Government nor any agency thereof, nor any of their employees, makes any warranty, express or implied, or assumes any legal liability or responsibility for the accuracy, completeness, or usefulness of any information, apparatus, product, or process disclosed, or represents that its use would not infringe privately owned rights. Reference herein to any specific commercial product, process, or service by trade name, trademark, manufacturer, or otherwise does not necessarily constitute or imply its endorsement, recommendation, or favoring by the United States Government or any agency thereof. The views and opinions of authors expressed herein do not necessarily state or reflect those of the United States Government or any agency thereof. Reference herein to any social initiative (including but not limited to Diversity, Equity, and Inclusion (DEI); Community Benefits Plans (CBP); Justice 40; etc.) is made by the Author independent of any current requirement by the United States Government and does not constitute or imply endorsement, recommendation, or support by the United States Government or any agency thereof.

OAK RIDGE National Laboratory

U.S. DEPARTMENT OF ENERGY

GSA

Prepared for the U.S. General Services Administration and the
U.S. Department of Energy

By Brian Fricke and Mahabir Bhandari

October 2019

Laboratory Evaluation and Field Demonstration of High Rotor Switched Reluctance Motor Technology

Disclaimer

The work described in this report was funded by the U.S. General Services Administration and the U.S. Department of Energy (DOE) under Contract No. 47PA0117C0005.

Acknowledgments

United States General Services Administration (GSA) Region 9 (San Ysidro Land Port of Entry): Jeremy Sawicki, Paul Knabe, and Mike Green

GSA Proving Ground Program (GPG): Michael Hobson and Kevin Powell

Oak Ridge National Laboratory: Heather Buckberry, Mark Adams, and Tony Gehl

Software Motor Company: David Miles, Trevor Creary, and Shams Shaikh

North Carolina Advanced Energy Corporation: Kitt Butler and Michael Lyda

For more information contact:

Brian Fricke
Oak Ridge National Laboratory

Email: frickeba@ornl.gov

The General Services Administration's GSA Proving Ground Program and DOE's High Impact Technology (HIT) Catalyst program enable federal and commercial building owners and operators to make sound investment decisions in next-generation building technologies based on their real-world performance.

Executive Summary

In this project, a new motor technology based on a novel design called a High Rotor Pole Switched Reluctance Motor (HRSRM) was demonstrated and evaluated. The HRSRM system combines an innovative electric motor design with a programmable variable-speed drive and a controller that provides real time monitoring and cloud-based connectivity. Unlike induction or permanent-magnet motor designs, this motor uses a switched reluctance (SR) design that purports to be simpler to manufacture and more reliable and efficient to operate.

Several of the stated benefits of the HRSRM system were evaluated as part of this project. First, the technology is claimed to offer greater energy efficiency than any motor currently on the market. Second, according to the manufacturer, the motor can be dropped into an existing pump or heating, ventilation, and air-conditioning application in less than 30 minutes, and has controls that can be pre-programmed to interact with the application's existing control structure. Third, the control system allows the HRSRM to replace a constant-speed motor with one that provides variable-speed capabilities without requiring the installation of a variable-speed drive.

The evaluation of a 10 hp HRSRM system was conducted in two parts. One portion of the evaluation consisted of performance tests conducted in a tightly controlled laboratory environment in which the performance of the HRSRM system was compared with that of a premium efficiency induction motor with a variable-frequency drive. The other portion of the evaluation was conducted at a field location within a General Services Administration facility in which the HRSRM system replaced an existing motor system in a 10 hp chilled water pump. The performance of the HRSRM system was compared with that of the incumbent motor system that was supplied with the pump from the manufacturer. The overall project and performance objectives for this motor evaluation are defined in Table ES.1.

Table ES.1. Performance Objectives

Objective	Success criteria	Metrics and data	Measurement and verification results
Energy savings—laboratory evaluation	>5% energy savings relative to baseline	Compare measured input and output power of HRSRM with that of state-of-the-art variable-speed induction motor	Met—efficiency gain of up to 11.4% achieved
Energy savings—field evaluation	>5% energy savings relative to baseline	Compare measured power consumption of HRSRM on a chilled water pump with that of incumbent motor at site. Metric is motor/drive power versus hydraulic power	Not met—energy savings of 4% achieved
Maintenance cost	No increase in maintenance costs for HRSRM system	Compare maintenance records for incumbent pump motor with records documenting cost of maintaining new pump motor	Met—no increase in the maintenance cost
Drop-in replacement capability	No physical modifications needed during installation	Determine if all connection points of HRSRM motor fit with existing connection points	Met—no modifications required during installation
Economic viability	<3-year simple payback period	Track installation (labor, parts, material) and operating costs (energy, maintenance) for both HRSRM and incumbent technologies	Not met—14.8 years
Ease with which HRSRM controls engage existing controls	Positive feedback from site operations and maintenance (O&M) staff indicates that the HRSRM system presented no unique challenges during installation and operation with site controls system	Site O&M staff maintain notes during installation and programming of HRSRM	Met—no challenges noted during operation with existing controls

During the laboratory evaluation of motor performance, both a 10 hp HRSRM and a National Electrical Manufacturers Association (NEMA) premium efficiency 10 hp induction motor were evaluated under the same operating conditions for a variety of motor loads and speeds. At each combination of speed and load, the following data were recorded:

- Speed (RPM)
- Torque (N·m)
- Input electrical power (W)
- Current (A)
- Voltage (V)
- Ambient temperature (°C)
- Motor case temperature (°C)

Based on these measurements, motor output power and motor efficiency were calculated.

At full rated speed and over the operating torque range for this speed, it was found that the HRSRM/drive was more efficient than the baseline motor/drive. At full rated speed, the maximum efficiency of the HRSRM/drive was 92.2%, which occurred at 90% full load torque, corresponding to a power output of 9.2 hp. The maximum efficiency of the baseline motor/drive at full rated speed was 89.4%, occurring at 60% full load torque, corresponding to a power output of 6.1 hp. Furthermore, on average, over the drive frequency range of 20 to 60 Hz, the HRSRM was found to be 4.5% more efficient than the baseline motor. The range of efficiency gain for the HRSRM compared with the baseline motor was between 1.5 and 11.4%.

The field validation portion of this project consisted of the evaluation of a 10 hp HRSRM in a pumping application that was a part of a chilled water distribution system at the General Services Administration's San Ysidro Land Port of Entry facility in San Ysidro, CA. During this evaluation, the following specific points of the pumping system were measured:

- Electric power input to the pump motor/drive (kW);
- Chilled water volumetric flow rate (gallons per minute, or GPM);
- Chilled water pressure at the pump inlet (pounds per square inch gauge, or psig); and
- Chilled water pressure at the pump outlet (psig).

Based on these measurements, the hydraulic power delivered by the motor/pump system was calculated and the overall pump system efficiency was determined.

Data were collected from the chilled water pump station during the month of August 2018 for the HRSRM/drive and during the month of September 2018 for the baseline motor/drive. For a given mode of operation in the field, the HRSRM/drive system was found to provide approximately 3.7 to 5.3% better efficiency compared with the baseline motor/drive system. However, during extended operation in the field, the HRSRM/drive system operated for an extended period of time in a lower efficiency mode of operation, thereby reducing any efficiency benefits that the HRSRM/drive system achieved.

An annual energy analysis was performed comparing the two motors on an equal basis using the field-measured performance data. To estimate the annual energy savings in the pumping application, the

pumping system behavior exhibited by the baseline motor/drive system was used as the basis for comparison. The annual energy savings associated with the HRSRM/drive for this pumping application is estimated to be 1,300 kWh, or 4%. In addition, assuming an average cost of electricity for commercial customers in California of $0.1759/kWh[1], the annual energy cost savings for the HRSRM retrofit is estimated to be $230.

The process of installing the HRSRM at the field test site was no different from that required for any other motor. Since the HRSRM complies with the NEMA 215T frame size, the HRSRM was easily bolted directly to the existing pump assembly and the motor shaft was easily coupled to the pump shaft. Immediately upon starting the HRSRM, and subsequently during its operation, it was noted that the HRSRM was significantly louder than the original pump motor, and facilities staff expressed concern that hearing protection would be required for performing work for extended periods of time near the HRSRM/drive. During the period for which the HRSRM/drive was operational in the chiller pump application; there were no reports of occupant dissatisfaction with the internal environment (*i.e.*, temperature and humidity) of the building spaces served by the chiller.

[1] EIA. 2018. Electric Power Monthly with Data for September 2018. U.S. Energy Information Administration, U.S. Department of Energy (DOE), Washington, D.C.

Table of Contents

I. Introduction

A. WHAT WE STUDIED

The objective of this U.S. General Services Administration (GSA) Proving Ground project is to evaluate the performance of the high rotor pole switched reluctance motor (HRSRM) system. The vendor's principal claim is that the HRSRM system is the "most energy efficient commercial production motor system in the world." Other claims by the vendor include the following:

- The HRSRM system is a drop-in replacement for other variable- and constant-speed motors.
- The HRSRM system incorporates a control method that is user friendly and easily interfaces with existing building control systems.

The results of this project will provide GSA with fundamental knowledge regarding the effectiveness of applying this energy-efficient motor in federal buildings. The results could also provide a roadmap that will guide GSA's decision making and policy regarding electric motors for years into the future. This project will provide GSA with critical data and information needed to modify and optimize its recommendations for electric motor replacement within the federal sector to leverage greater energy savings available from using the highest-efficiency motors on the market.

B. WHY WE STUDIED IT

Heating, ventilation and air conditioning (HVAC) represents more than 40% of GSA's electrical energy spending, with electric motors (*e.g.*, for compressors, pumps, fans, etc.) representing more than 60% of the HVAC electrical energy cost. With standardized motor sizes providing drop-in replacement, and with efficiencies 5% greater than current premium efficiency electric motors at their rated (full) speeds—and up to 30% greater at part loads and speeds—smart switched reluctance (SR) motor technology has the potential to provide GSA with significant energy cost savings. Furthermore, integrated sensing and reporting, out-of-the-box variable-speed capability, and easy configuration of smart motor systems promise additional operations and maintenance (O&M) savings.

II. Evaluation Plan

A. TECHNOLOGY DESCRIPTION

All electric motors function as converters of electrical energy to magnetism and then to mechanical rotating motion. The operation of all electric motors is based on the interaction between a field magnet and a magnetic rotor. The electromagnetic interactions between these two magnets cause the rotor to rotate. The different types of motors result from the manner in which the rotating magnetic fields are generated.

Induction Motor

In a traditional induction motor, alternating current is fed into the stator coil, which creates a rotating magnetic field around the stator. This rotating magnetic field in the stator induces a current in the rotor coil, which, in turn, generates a magnetic field around the rotor. The magnetic fields of the rotor and stator interact. As the magnetic field in the stator rotates, the rotor follows it and torque is generated.

Fig. 1 shows the stator coil and rotor configuration for an induction motor. The core of the rotor consists of steel laminations with grooves around the periphery. Copper or aluminum bars are set within these grooves, running the length of the rotor. Shorting rings are located at each end of the rotor. Because of the cage-like shape of the rotor, it is often referred to as a squirrel-cage rotor.

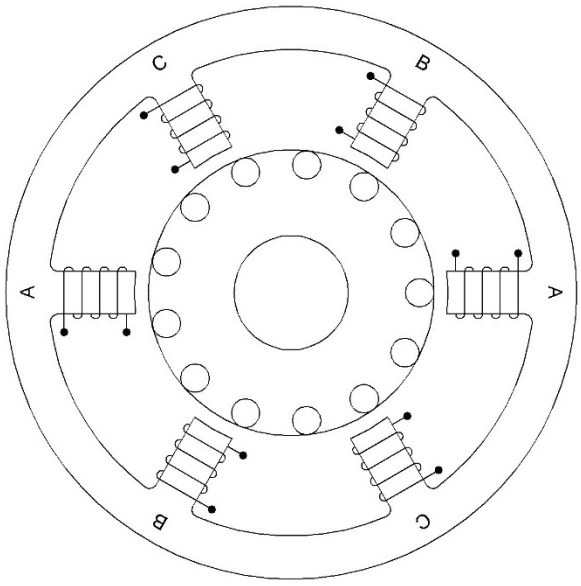

Fig. 1. Stator and rotor configuration in an induction motor.

High Rotor Pole Switched Reluctance Motor

The new technology demonstrated in this project is based on a novel design, the HRSRM. The HRSRM system combines an innovative electric motor design with a programmable variable-speed drive and a controller that provides real time monitoring and cloud-based connectivity. Unlike induction or permanent-magnet motor designs, which have barely changed in more than a century, this motor uses an SR design that purports to be simpler to manufacture and more reliable and efficient to operate. This motor claims extremely high operational efficiencies of over 90% in HVAC fan/blower types of applications across a wide range of speeds and torques, plus sensing and control software that can reduce electricity consumption by over 30%.

A traditional switched reluctance motor (SRM) consists of a stator whose poles have windings to form electromagnets. In addition, the rotor has poles that do not have windings. When the coils on opposite stator poles are energized, the stator and rotor poles line up and a magnetic circuit with low reluctance (resistance) is formed. This configuration is illustrated in Fig. 2, in which the stator coils "A" are energized, and the rotor poles "1" and "4" line up with the stator poles "A". Sequentially switching currents in the stator windings will change the magnetic circuit formed by the stator and rotor, and the rotor will follow the moving magnetic field from the stator poles to minimize the reluctance, thereby producing rotation and torque.

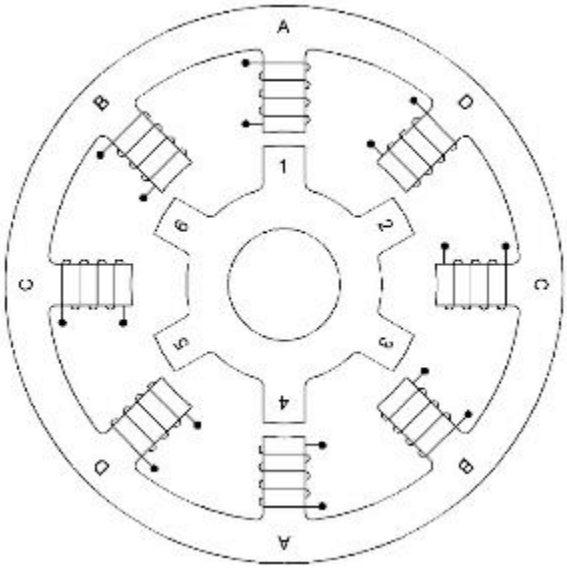

Fig. 2. Stator and rotor configuration in a switched reluctance motor.

For the SRM to produce torque, there must be different numbers of stator poles and rotor poles; otherwise, all the stator poles and rotor poles would line up and no rotation would occur. Traditional SRMs have more poles on the stator and fewer on the rotor, as shown in Fig. 2. However, an HRSRM, such as the one produced by SMC, has more poles on the rotor and fewer on the stator, as shown in Fig. 3. An exploded view of the SMC HRSRM is shown in Fig. 4, in which the design and layout of the rotor and stator coils are illustrated.

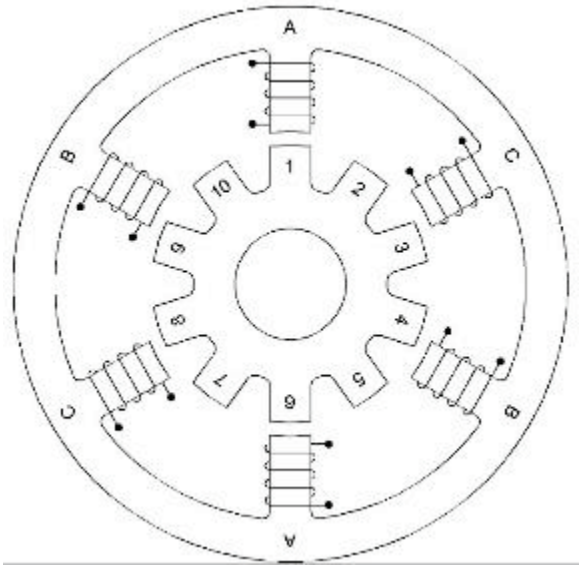

Fig. 3. Stator and rotor configuration in a high rotor pole switched reluctance motor.

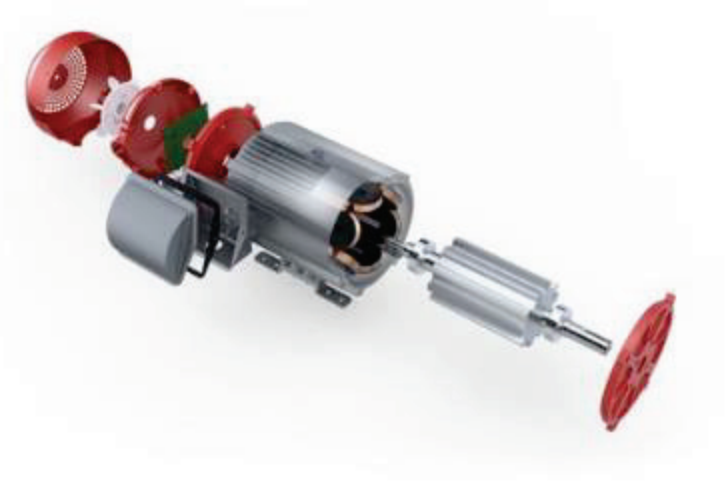

Fig. 4. Configuration of the high rotor pole switched reluctance motor.

The advantages of the HRSRM versus a typical induction motor include the following:

- Simple and robust construction: The HRSRM rotor design is simpler than that of the squirrel cage rotor because it consists only of laminations with no windings or conductor bars. Furthermore, the HRSRM stator consists of simple electromagnets.
- Lack of electrical current in the rotor: Since no electrical current is induced in the HRSRM rotor, there is no electrical arcing across the motor bearings and, thus, premature bearing failure is eliminated.
- Higher efficiency compared with induction motors: Note that traditional SRMs are generally not more efficient than induction motors; however, as a result of the HRSRM's patented motor design, the HRSRM is more efficient than an induction motor.
- Use of power electronics to drive motor, which allows for precise motor control.

The disadvantages of HRSRM compared with a typical induction motor include the following:

- Requires power electronics to drive the motor, which increase the cost if the HRSRM replaces a fixed-speed induction motor. However, if it is compared with a variable-speed induction motor, the cost of the induction motor and its variable-frequency drive (VFD) will be comparable to the cost of the HRSRM motor and drive.
- The HRSRM model produced for this demonstration produces more audible noise, since the magnetic forces tend to pull the stator toward the rotor.

Motor Efficiency

The efficiency of a motor is defined as the ratio of its mechanical power output to its electrical power input. The major causes of inefficiency in a motor include core losses, friction and windage losses, stator resistance losses, rotor resistance losses, and stray load losses.[2] The design and construction of a motor influence the magnitude of these losses. Motor losses ultimately manifest themselves as heat, which is dissipated to the surroundings. In facilities with large motor loads, this heat may represent a sizable load on building HVAC systems.

- Core losses are associated with the energy required to overcome the resistance to changing magnetic fields within the core material.
- Windage and friction losses are associated with the energy required to overcome bearing friction and air resistance within the motor.
- Stator losses are due to current flow through the stator winding and appear as heating due to the resistance of the winding.
- Similarly, rotor losses are due to current flow through the rotor winding and appear as heating due to the resistance of the windings.
- Stray load losses are the result of leakages fluxes induced by load currents.

[2] U.S. DOE. 2014. *Premium Efficiency Motor Selection and Application Guide: A Handbook for Industry*. Advanced Manufacturing Office (AMO), Office of Energy Efficiency and Renewable Energy (EERE), DOE, Washington, D.C.

Induction motors operate relatively efficiently, with typical efficiencies in the range of 80 to 94%[2]. In general, motor efficiency increases with increasing motor size. In addition, the potential for improving motor efficiency is much greater for motors of smaller power ratings.

The Energy Policy Act (EPAct) of 1992 required that most general-purpose motors manufactured for sale in the United States after October 24, 1997, meet the NEMA Energy Efficient Motor Standard. In August of 2001, the National Electrical Manufacturers Association (NEMA) adopted the NEMA Premium Motor Standard, which was more stringent than the older Energy Efficient Motor Standard. Fig. 5 shows the NEMA energy efficiency and premium efficiency motor standards for four-pole (1,800 RPM) motors as a function of motor power rating for the range of 1 to 25 hp. Subsequently, the EPAct of 2005 mandated the purchase and use of premium efficiency motors at all federal facilities.

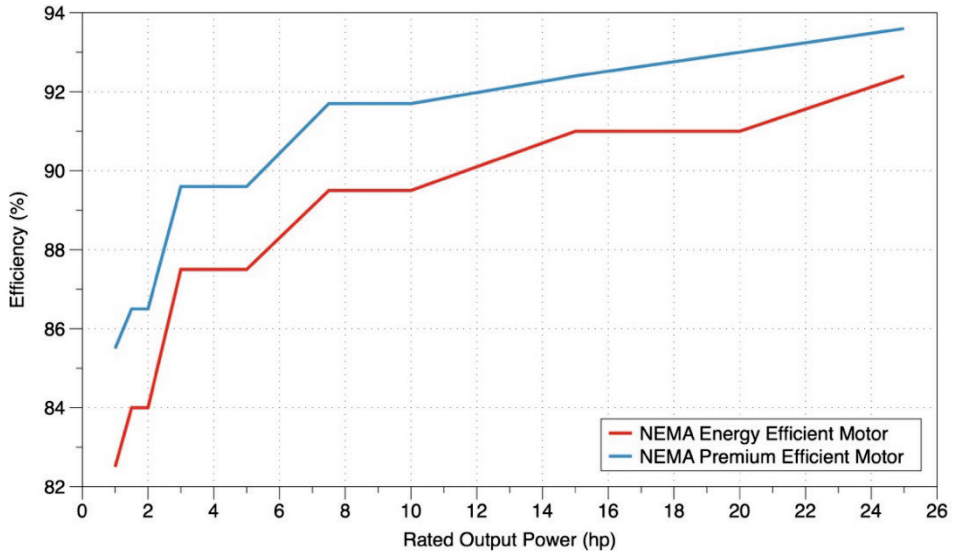

Fig. 5. Efficiencies of NEMA energy efficiency and premium efficiency motors.[3]

[3] ANSI/NEMA. 2016. ANSI/NEMA MG 1-2016, Motors and Generators. National Electrical Manufacturers Association, Rosslyn, Virginia.

B. EVALUATION DESIGN

Several of the stated benefits of the HRSRM system were evaluated as part of this project. First, the technology is claimed to offer higher energy efficiency than any motor currently on the market. Second, the motor can be "dropped-in" to an existing pump or HVAC application in less than 30 minutes and has controls that can be pre-programmed to interact with the application's existing control structure. Third, the control system allows the HRSRM to replace a constant-speed motor with one that provides variable-speed capabilities, but without the typical requirement for a variable-speed drive.

The evaluation of the HRSRM system was conducted in two parts. One portion of the evaluation consisted of performance tests conducted in a tightly controlled laboratory environment in which the performance of the HRSRM system was compared with that of a current state-of-the-industry variable-speed induction motor. The other portion of the evaluation was conducted at the San Ysidro Land Port of Entry (LPOE), San Ysidro, CA, where the HRSRM system was installed as a drop-in replacement for an existing motor system in a 10 hp chilled water pump. The performance of the HRSRM system was compared with that of the incumbent motor system supplied with the pump by the manufacturer. The success criteria for the motor system evaluation are defined in Table 1.

Table 1. The quantitative objectives and performance objective

	Metrics and data	Success criteria
Quantitative Objectives		
Energy savings	Laboratory evaluation: Measure power consumption and other parameters of HRSRM across pre-determined set of operating conditions. Compare with state-of-the-art variable speed induction motor	>5% energy savings relative to baseline
	Field evaluation: Measure power consumption of HRSRM across range of operation on a chilled water pump. Compare with performance of incumbent motor at site. Metric is motor/drive power versus hydraulic power of pump	>5% energy savings relative to baseline
Maintenance cost	Compare maintenance records for incumbent pump motor with records documenting cost of maintaining new pump motor	No increase in maintenance costs for HRSRM system.
Drop-in replacement capability	During motor replacement at field location, determine if all connection points of new motor fit with existing connection points	No physical modifications needed during installation
Economic viability	Track all installation (labor, parts, material) and operating costs (energy, maintenance) for both HRSRM and incumbent technologies	<3-year simple payback period
Qualitative Objectives		
Ease with which HRSRM controls engage existing controls	Site operations and maintenance (O&M) staff maintain notes during installation and programming of HRSRM	Positive feedback from site O&M staff indicating that the HRSRM system presented no unique challenges during installation and operation with site controls system

C. DESCRIPTION OF DEMONSTRATION SITE

The HRSRM technology was demonstrated at the LPOE facility in San Ysidro, CA. This facility is the most active border crossing between the United States and Mexico and is located approximately 20 miles south of San Diego, CA (see Fig. 6). The facility's HVAC system is served by a chilled water distribution system. The new HRSRM/drive technology was evaluated on a chilled water pump located in the Head House of the San Ysidro LPOE facility (see Fig. 7).

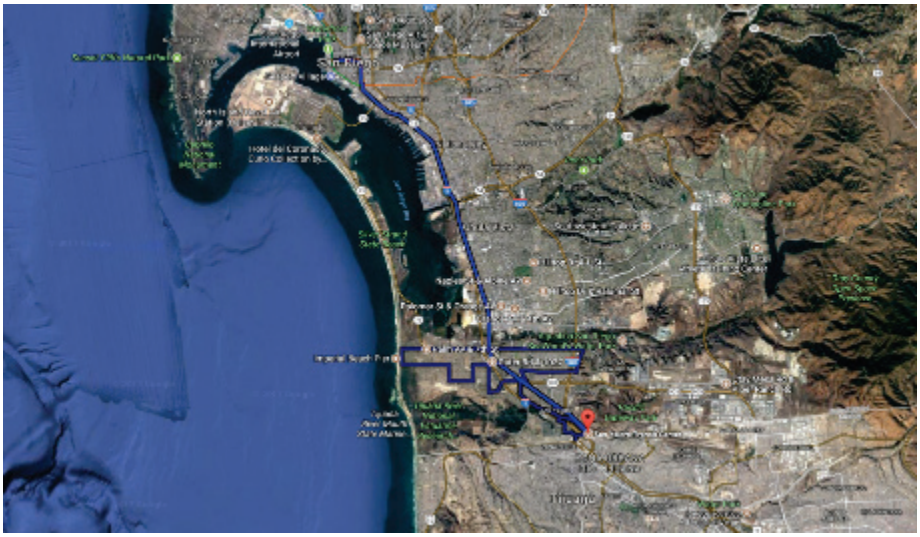

Fig. 6: San Ysidro LPOE location relative to San Diego, CA.

Fig. 7: Detail of the demonstration site. Actual location of the field demonstration is the smaller of the two buildings shown in the center-left of the image.

D. METHODOLOGY

Laboratory Performance Evaluation

The details of the experimental setup used to evaluate the performance of the HRSRM technology under tightly controlled laboratory conditions are given in Appendix A, and a summary of the setup is provided here. This laboratory performance evaluation was conducted by North Carolina Advanced Energy Corporation (Raleigh, NC) with observation and guidance from Oak Ridge National Laboratory (ORNL) staff. Both the HRSRM and a NEMA premium efficiency induction motor were evaluated under the same operating conditions for a variety of motor loads and speeds determined by the project team. The measured performance of the induction motor served as a baseline to determine the improvements in performance that could potentially be provided by the HRSRM.

A 10-hp Baldor motor (model EM3774T) and a Yaskawa VFD (model CIMR-AU4A0018FAA) were used to provide the baseline data for comparison with the 10 hp HRSRM (SMC model V03-1000-4-D00) and drive (SMC model SMC-P05-EX). The HRSRM drive was pre-programmed by the manufacturer before the evaluation and no changes were made to the drive's parameters. The Yaskawa VFD was operated in the volts/hertz mode; only those parameters specific to the Baldor motor nameplate were changed from the default, and all other VFD default parameters were used.

Each motor was mounted and aligned to a dynamometer. A precision power analyzer was used to measure the electrical input (voltage, current, and real power) to each motor drive. In addition, a torque transducer was used to record the mechanical output at the shaft of each motor. Finally, motor casing temperature and ambient temperature were measured throughout the testing. A schematic of the test setup is shown in Fig. 8.

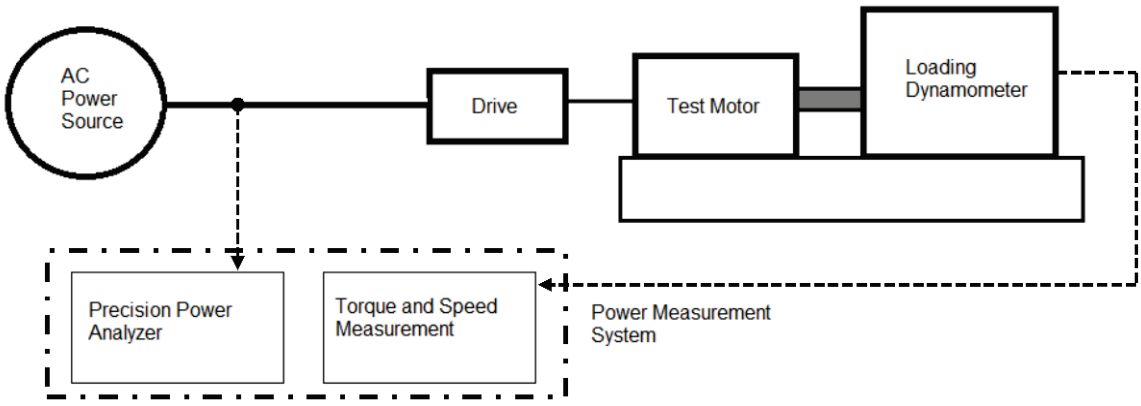

Fig. 8. Schematic of the motor dynamometer test setup (North Carolina Advanced Energy Corporation).

Each motor was operated at 9-speed and 10-torque settings, as indicated by the test matrix shown in Table 2. This gives a matrix of 90 different conditions for each motor/drive combination. At each combination of speed and torque, the following data were recorded:

- Speed (RPM)
- Torque (N·m)
- Input electrical power (W)
- Current (A)
- Voltage (V)
- Ambient temperature (°C)
- Motor case temperature (°C)

Based on these measurements, motor output power and motor efficiency were calculated. The torque set points shown in Table 2 were calculated as a percentage of the rated full load torque of the Baldor induction motor, and these same torque values were used for evaluating the HRSRM motor.

Table 2. Test matrix for laboratory motor performance evaluation

Torque	Frequency (Hz)								
(%)	60.0	53.3	46.7	40.0	33.3	26.7	20.0	13.3	6.7
100									
90									
80									
70									
60									
50									
40									
30									
20									
10									

Field Performance Evaluation

The field validation portion of this project consisted of the evaluation of the HRSRM at a field location within a GSA facility. This evaluation was conducted on a pumping application that was part of a chilled water distribution system at GSA's San Ysidro LPOE facility. During this evaluation, the following specific points of the pumping system were measured:

- Electric power input to the pump motor/drive (kW)
- Chilled water volumetric flow rate (GPM)
- Chilled water pressure at the pump inlet (psig)
- Chilled water pressure at the pump outlet (psig).

As part of the field evaluation, ORNL supplied instrumentation to measure the parameters listed for the existing motor and pump (to gather baseline data), as well as for the HRSRM retrofit. After the performance of the baseline induction motor was measured for several months, the incumbent induction motor and drive were retrofitted with the HRSRM and its associated drive.

Determination of Hydraulic Power

During the field evaluation of the motor systems, the key performance parameters for each motor included the electrical power supplied to the VFD or inverter of each motor and the hydraulic power delivered by the pump into the chilled water system. These data points were gathered in 5-minute intervals for each motor, and the data gathered at each of these 5-minute intervals reflected the **average** value of that data point over the past 5 minutes.

Hydraulic power is not a parameter that can be measured directly at the pump. Rather, it is calculated by measuring the pressure at the pump inlet and outlet, as well as the chilled water flow rate through the pump. Hydraulic power,$\dot{W}_{hydr}$, can be calculated as follows:

$$\dot{W}_{hydr} = \dot{m}h\,,$$

where $\dot{m}$ is the mass flow rate of the chilled water and h is the differential head across the pump.

The ultrasonic flow meter used during the field study provided the volumetric flow rate of the chilled water in units of GPM. To convert volumetric flow rate to mass flow rate, it was assumed that the density of the chilled water was 62.4 lb_m/ft^3. The pressure transducers that were used to provide the pressure difference across the pump provided pressure values in psig. To convert pressure difference to head, it was assumed that 1 psig is equivalent to 2.31 ft of water column. Noting that 1 hp is equivalent to 550 ft·lb/s, the hydraulic power delivered by the pump can be obtained from the measured volumetric flow rate and pressure difference as follows:

$$\dot{W}_{hydr} = \frac{Q\Delta P}{1714}\,,$$

where $\dot{W}_{hydr}$ is the hydraulic power (hp) delivered by the pump, Q is the volumetric flow rate of the chilled water (GPM), and ΔP is the pressure differential across the pump (psi). The overall efficiency of the motor/drive/pumping system, η, can then be determined as follows:

$$\eta = \frac{\dot{W}_{hydr}}{\dot{W}_{in}}\,,$$

where $\dot{W}_{in}$ is the electrical power supplied to the pump motor/drive.

Measurement Setup and Technology Deployment

The two stages of deployment for the motor performance evaluation consisted of the following:

- Establishing a baseline by collecting measurements for a 1-month period with the existing motor/drive; and
- Removing the existing motor/drive, deploying the HRSRSM/drive, and collecting retrofit measurements for a 1-month period.

Baseline

The chilled water pump selected for the field demonstration serves three air handing units in the San Ysidro facility. The pump was manufactured by Bell & Gossett and was rated to supply 600 GPM at a head of 37 feet of water. The recommended motor for the pump is a 10 hp motor operating at 1800 RPM. As originally installed at the San Ysidro facility, the pump used a Baldor Reliance SuperE induction motor (Model EM3774T) rated at 10 hp and 1760 RPM, with a VFD manufactured by ABB (Model ACH550), rated at 480 V, 15.4 A.

To determine the performance of the baseline pumping system with the Baldor motor and ABB drive, the following sensors were installed; these measurements points are illustrated in Fig. 9.

- Power meter and current transformers (CTs) to measure electric power input to the motor/drive (kW);
- Ultrasonic flow meter to measure chilled water volumetric flow rate (GPM);
- Pressure transducer to measure chilled water pressure at the pump inlet (psig); and
- Pressure transducer to measure chilled water pressure at the pump outlet (psig).

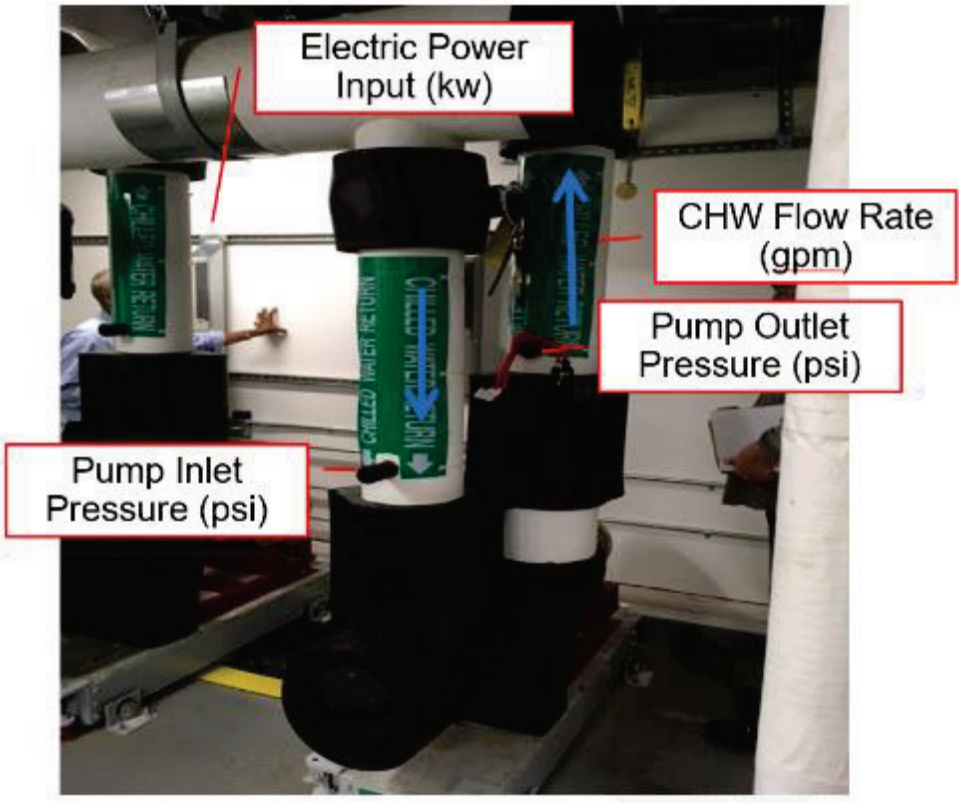

Fig. 9: Field measurement points.

The specifications of the instrumentation installed at the test site are summarized in Table 3. An uncertainty analysis indicates that the pump system efficiency, η, can be calculated from the measured data to within ±0.01.

Table 3. Instrumentation specifications

Instrument	Measured quantity	Instrument range	Accuracy
Power meter (Continental Control Wattnode WNB-3D-480-P Accu-CT ACTL-0750-20	Motor/drive input power	0–20 amps	±0.5% of reading
Pressure transducer (Ashcroft T27M0242EW200)	Chilled water pump inlet and outlet pressures	0–200 psi	±0.25% of full scale
Ultrasonic flow meter (Micronics U3000)	Chilled water flow rate	0.33 ft/s to 65.62 ft/s	±0.5 to ±2.0% of flow reading for flow rate >0.66 ft/s and pipe ID >2.95 in

A Campbell Scientific CR6 datalogger with a 24-bit analog-to-digital converter was selected for making the analog sensor measurements. The logger was programmed to scan all sensors at 1-sec intervals. Data were then recorded at 1-min, 5-min, and 60-min intervals. A cellular modem was used to synchronize data from the datalogger installed at the site to a server at ORNL for archiving and analysis. A real-time data system was used to monitor and plot the measurements during testing at the San Ysidro field site. Note that the datalogger was used for monitoring only, and there was no control functionality.

Fig. 10 shows the locations of the pressure transducers measuring the inlet and outlet pressures of the pump. Fig. 11 shows the enclosures housing the power meter and data acquisition system, as well as the flow meter display/transmitter unit. Fig. 12 shows the location of the ultrasonic flow meter installed on the chilled water line. The flow meter was insulated to prevent condensation from forming on the meter.

Fig. 10. Locations of pressure transducers: (a) inlet pressure, (b) outlet pressure.

Fig. 11. Instrumentation: (a) power meter, (b) data acquisition system, (c) flow meter display/transmitter unit.

Fig. 12. Location of ultrasonic flow meter (red oval).

Retrofit

Following the baseline measurement period, the incumbent induction motor (Baldor) and its drive (ABB) were retrofitted with the HRSRM and its drive. The SMC motor (Model V03) is rated at 10 hp and 1800 RPM, and the SMC drive (Model SMC-P05-EX) is rated for 460V, 60 Hz, and 1.8 to 16 A. Fig. 13 shows the SMC drive, the original VFD (ABB), the power meter (in enclosure), the data acquisition system (in enclosure), the flow meter display/transmitter unit, and the SMC motor.

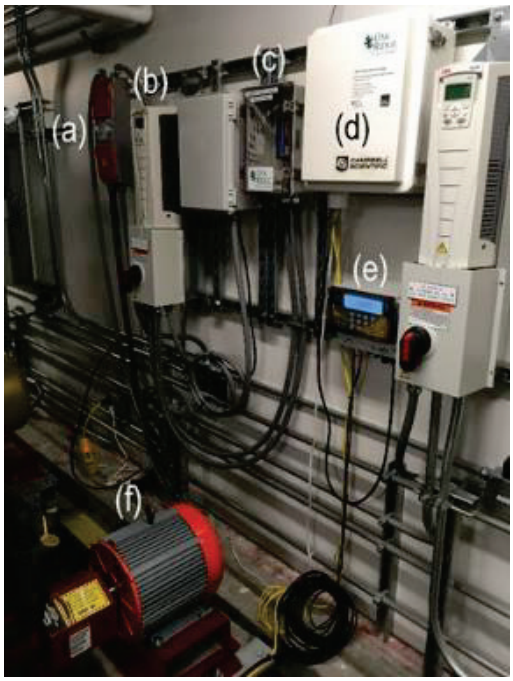

Fig. 13. Equipment and instrumentation for motor performance field demonstration: (a) SMC motor drive, (b) ABB motor drive, (c) power meter, (d) data acquisition system, (e) flow meter display/transmitter unit, (f) SMC motor.

III. Demonstration Results

Laboratory Evaluation Results and Analysis

The detailed results of the laboratory evaluation of the motor technologies, as performed by North Carolina Advanced Energy Corporation, are given in Appendix A, and a summary of these results is provided in this section. A comparison of the efficiency of the HRSRM/drive and the baseline motor/drive, both operating at a drive frequency of 60 Hz (full rated speed), is shown in Fig. 14. It can be seen that over the operating torque range for this speed, the HRSRM/drive was more efficient than the baseline motor/drive. At this speed, the maximum efficiency of the HRSRM /drive was 92.2%, which occurred at 90% full load torque, corresponding to a power output of 9.2 hp. The maximum efficiency of the baseline motor/drive was 89.4%, occurring at 60% full load torque, corresponding to a power output of 6.1 hp. On average, over the torque range for a drive frequency of 60 Hz, the HRSRM was 3.0% more efficient than the baseline induction motor. Finally, the maximum power output of both the HRSRM and the baseline induction motor occurred at 100% full load torque, with the HRSRM achieving a maximum power output of 10.2 hp, while the baseline induction motor achieved a maximum power output of 10.0 hp.

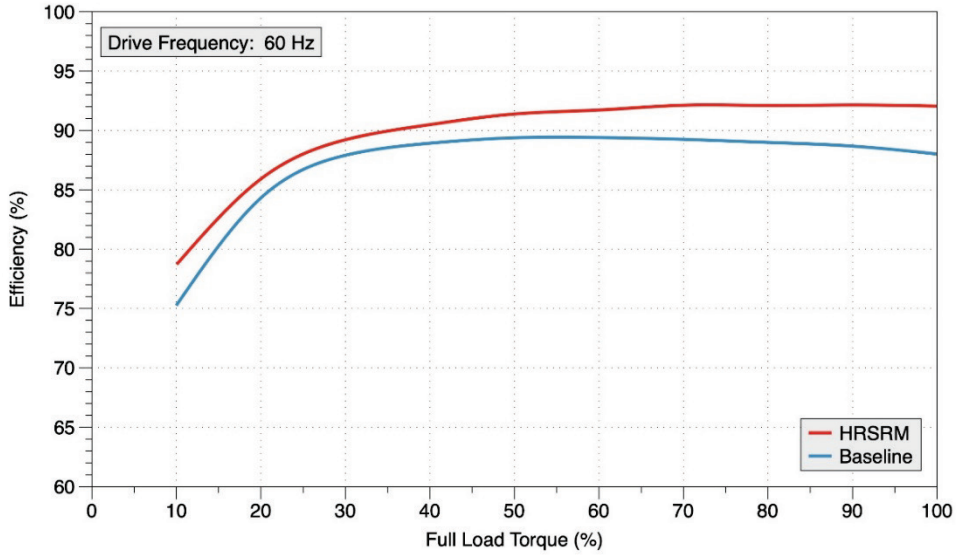

Fig. 14. Efficiency of the HRSRM/drive and the baseline motor/drive as a function of applied torque for a drive frequency of 60 Hz.

Similar plots of efficiency versus percentage full load torque are given in Fig. 15 for a drive frequency of 40 Hz and in Fig. 16 for a drive frequency of 20 Hz. It can be seen that for both the HRSRM/drive and the baseline motor/drive, efficiency decreases as drive frequency (and motor speed) decreases. Also, for any given load and motor speed, the HRSRM /drive exhibits higher efficiency than the baseline motor/drive.

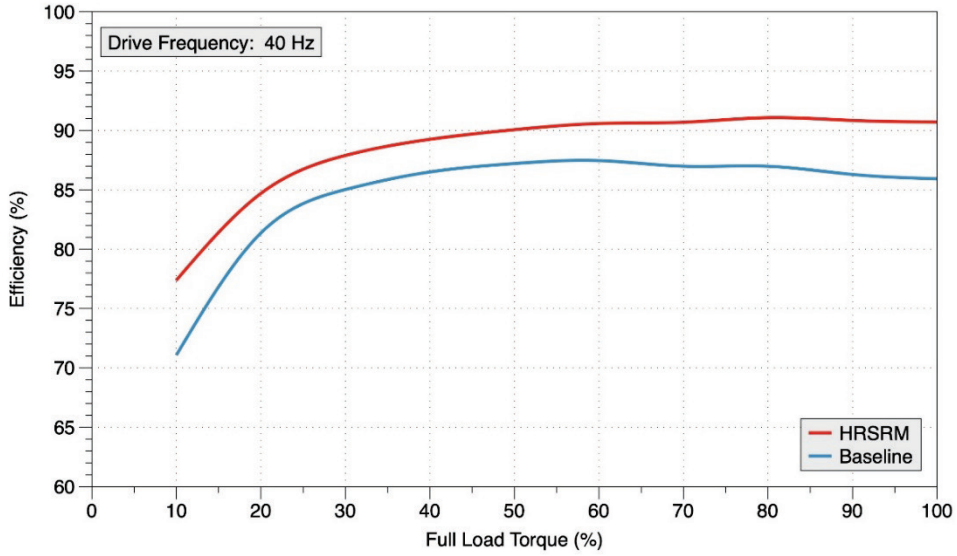

Fig. 15. Efficiency of the HRSRM/drive and the baseline motor/drive as a function of applied torque for a drive frequency of 40 Hz.

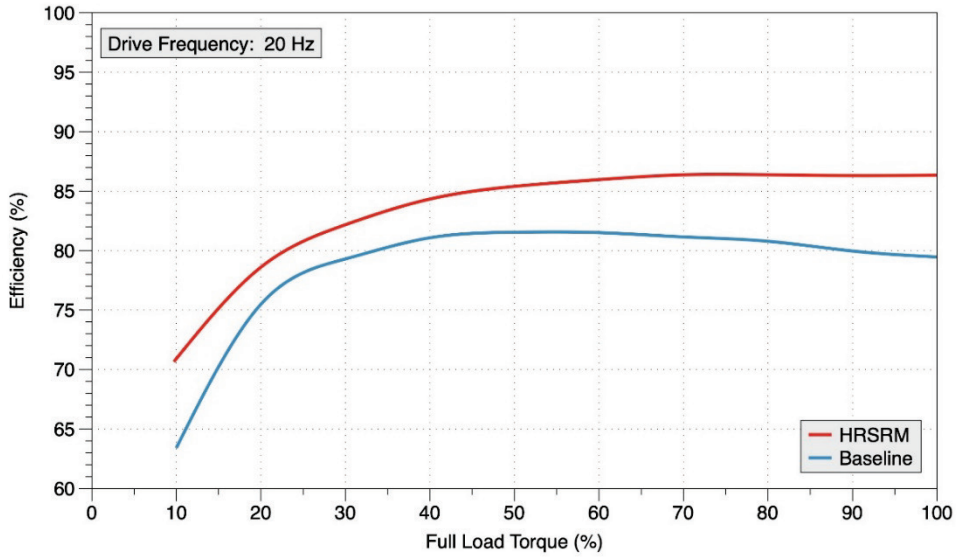

Fig. 16. Efficiency of the HRSRM/drive and baseline motor/drive as a function of applied torque for a drive frequency of 20 Hz.

Finally, the relative difference in efficiency between the HRSRM/drive and the baseline motor/drive is shown in Fig. 17. For a given motor speed and applied torque, the relative difference in efficiency is defined as follows:

$$\Delta\eta = \left(\frac{\eta_{HRSRM,i} - \eta_{baseline,i}}{\eta_{baseline,i}}\right) 100\% \,,$$

where $\Delta\eta$ is the relative difference in efficiency between the HRSRM and baseline motors, $\eta_{HRSRM,i}$ is the efficiency of the HRSRM motor/drive at a given operating condition, *i*, and $\eta_{baseline,i}$ is the efficiency of the baseline motor/drive at the same given operating condition, *i*.

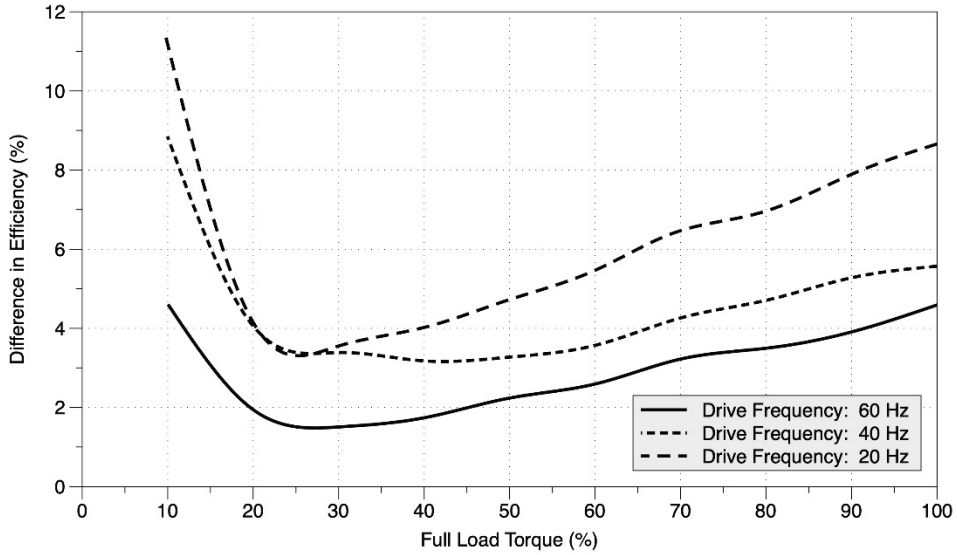

Fig. 17. Relative difference in motor efficiency between the HRSRM/drive and the baseline motor/drive, for drive frequencies of 60, 40, and 20 Hz.

It can be seen from Fig. 17 that the relative difference in efficiency between the HRSRM and baseline motors is the greatest at either the highest values of torque or the lowest values of torque. The minimum relative difference in efficiency between the HRSRM/drive and the baseline motor/drive occurs at around 25 to 30% of full load torque.

At a drive frequency of 60 Hz and 100% full load torque, the HRSRM is 4.6% more efficient than the baseline induction motor. Furthermore, as the motor speed decreases, the difference in efficiency between the two motors increases. At a drive frequency of 20 Hz and 100% full load torque, the HRSRM is 8.7% more efficient than the baseline motor.

On average, over the drive frequency range of 20 to 60 Hz, the HRSRM was found to be 4.5% more efficient than the baseline motor. The range of efficiency gain for the HRSRM was between 1.5 and 11.4%.

Field Evaluation Results and Analysis

Data collected from the chilled water pump station at the San Ysidro LPOE field site during the month of August 2018 for the HRSRM/drive, and during the month of September 2018 for the baseline motor/drive, were used to compare the performance of the two motor systems. As can be seen in Fig. 18 and Fig. 19, the ambient temperatures and total solar irradiation in the San Diego/San Ysidro area were similar for the months of August and September; thus, the demand on the chiller should be similar, resulting in similar chilled water pump behavior for the two months.

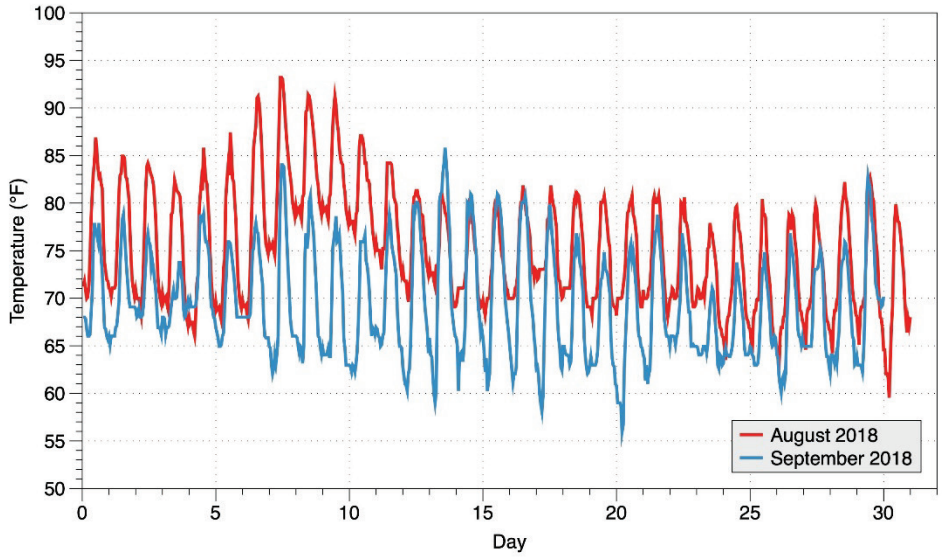

Fig. 18. Hourly ambient temperature for San Diego, CA, during August and September, 2018.

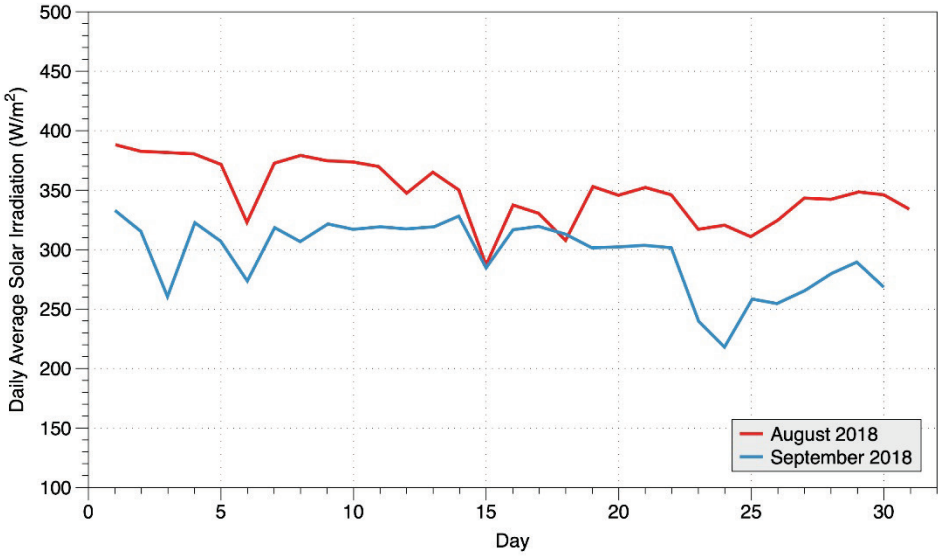

Fig. 19. Daily average solar irradiation for San Diego, CA, during August and September, 2018.

Fig. 20 shows the measured chilled water flow rate through the pump, and Fig. 21 shows the measured pressure differential across the water pump for August 2018 (HRSRM and drive) and September 2018 (baseline motor and drive). The chilled water flow rate was found to vary between 200 and 700 GPM, and the pump pressure differential varied between 8 and 16 psi. Based on the measured flowrate and pressure differential, the hydraulic power delivered by the water pump was calculated and is shown in Fig. 22. Hydraulic power was generally found to range from 1 to 5 hp.

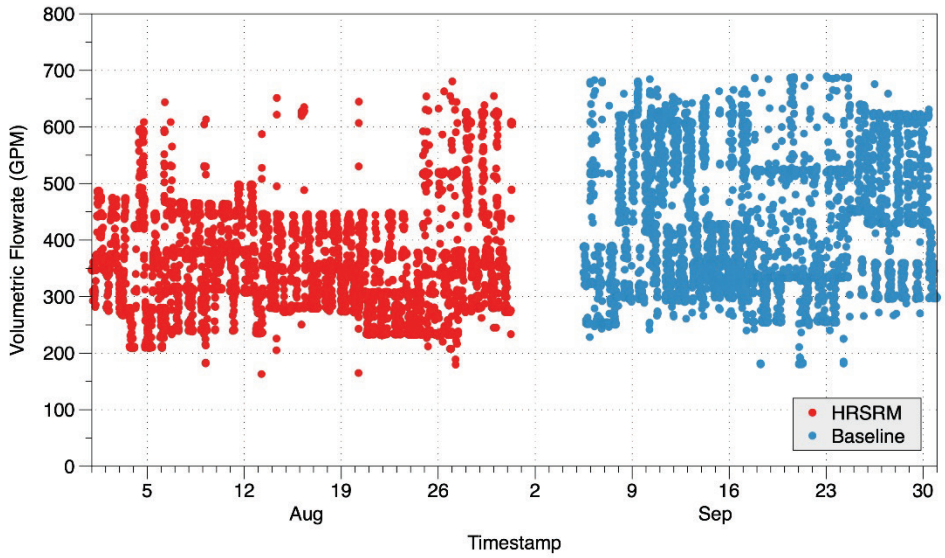

Fig. 20. Flowrate through the chilled water pump during August 2018 (HRSRM and drive) and September 2018 (baseline motor and drive).

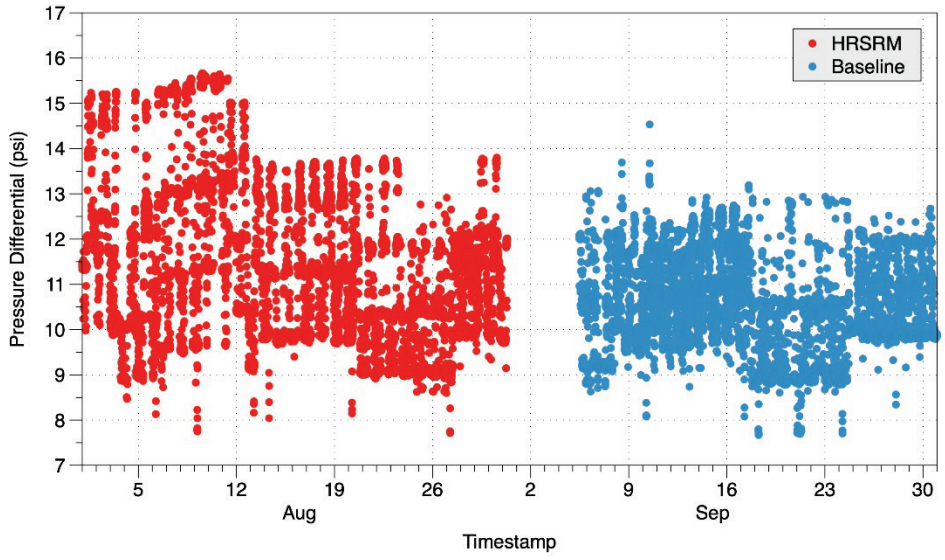

Fig. 21. Pressure differential across the chilled water pump during August 2018 (HRSRM and drive) and September 2018 (baseline motor and drive).

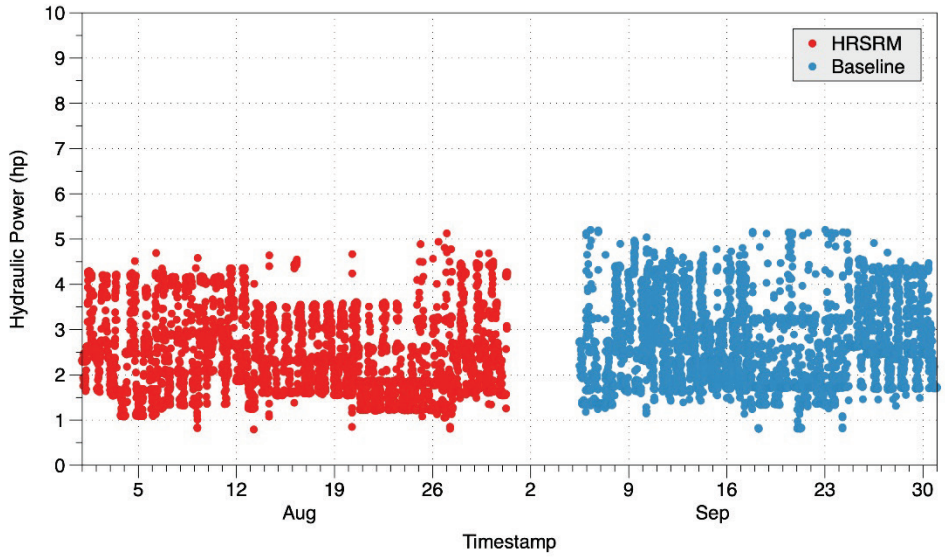

Fig. 22. Calculated hydraulic power delivered by the chilled water pump during August 2018 (HRSRM and drive) and September 2018 (baseline motor and drive).

The measured electrical input power to the two motor/drive systems is shown in Fig. 23; it was found to vary between 2 and 9 hp. By dividing the hydraulic power (*i.e.*, system output power) by the electrical input power (*i.e.*, system input power), the total pumping system efficiency was determined. The total pumping system efficiency, shown in Fig. 24, was found to range from roughly 45 to 65%.

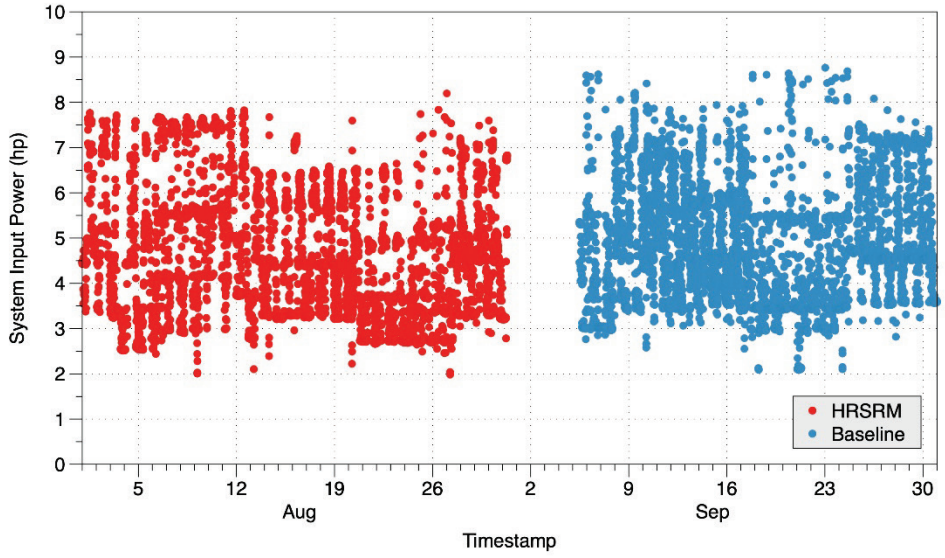

Fig. 23. Electrical input power supplied to the chilled water pump motor/drive during August 2018 (HRSRM and drive) and September 2018 (baseline motor and drive).

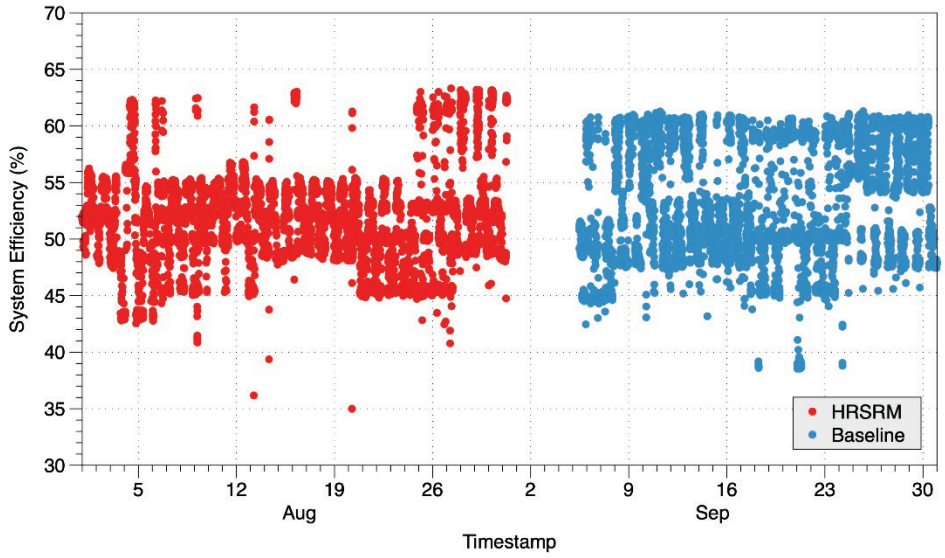

Fig. 24. Total pumping system efficiency during August 2018 (HRSRM and drive) and September 2018 (baseline motor and drive).

Pumping system efficiency versus calculated hydraulic power is plotted in Fig. 25. It can be seen that the pumping system exhibited one of two distinct trends, depending on whether the HRSRM/drive or the baseline motor/drive was used. Consider Fig. 26, in which the pressure differential across the pump is plotted versus hydraulic power. The two trends shown in Fig. 25 can easily be separated by the solid black line shown in Fig. 26. Data associated with the points above the line shown in Fig. 26 will be designated as the "high dP" operating mode, whereas those data associated with the points below the line shown in Fig. 26 will be designated as the "low dP" operating mode.

The two trends shown in Fig. 25 are separated in Fig. 27: low dP operation is shown in Fig. 27(a) and high dP operation in Fig. 27(b). It was found that the pumping system with the HRSRM/drive operated nearly 90% of the time in high dP mode and only 10% of the time in low dP mode. The pumping system with the baseline motor/drive spent a nearly equal amount of time operating in high dP and in low dP mode (48% in high dP mode and 52% in low dP mode). The discrepancy in the amount of time spent operating in the two modes by the two motors is unknown; however, it should be noted that during the course of this demonstration, the building cooling load serviced by the chiller increased significantly since a new building was brought on-line.

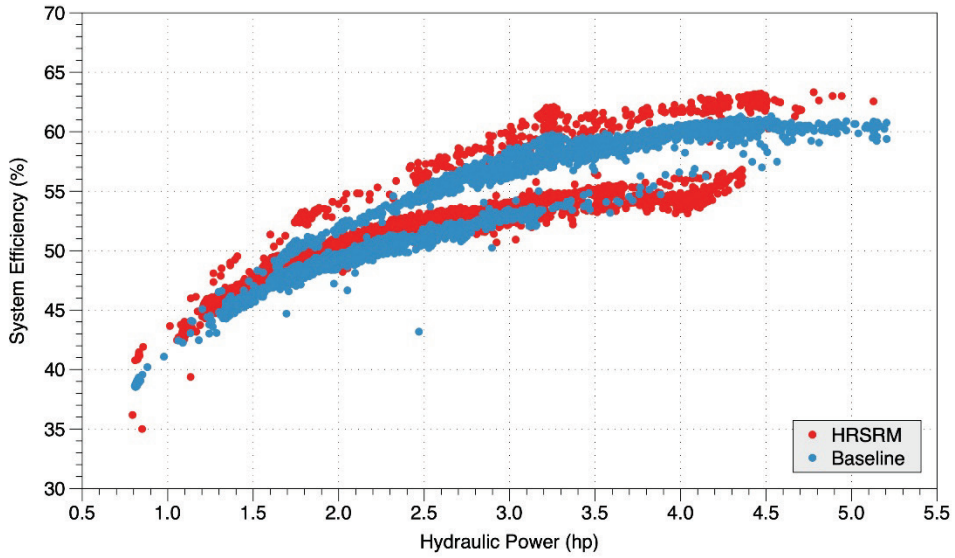

Fig. 25. Pumping system efficiency versus hydraulic power for the HRSRM/drive system and the baseline motor/drive system.

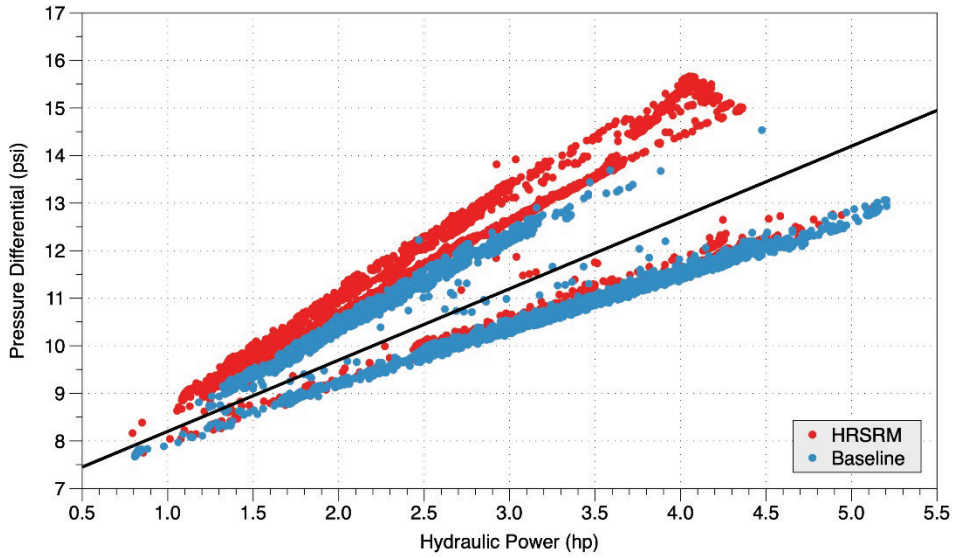

Fig. 26. Pressure differential versus hydraulic power for the HRSRM/drive system and the baseline motor/drive system.

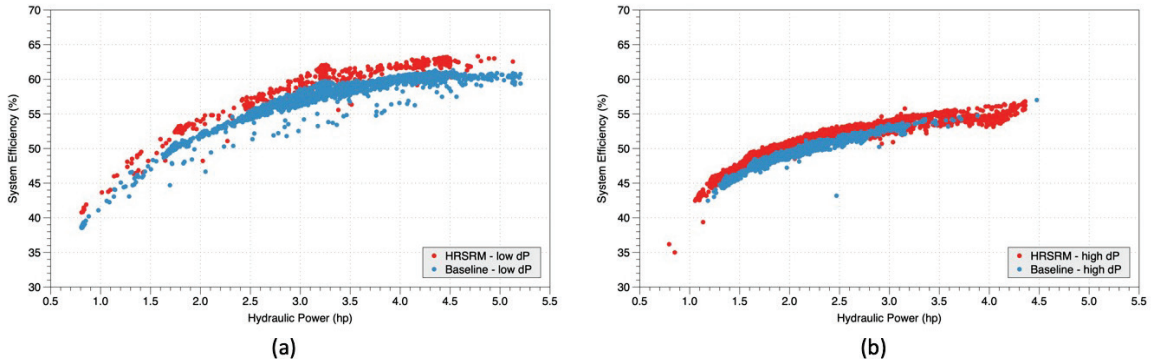

Fig. 27. Pumping system efficiency versus hydraulic power for the HRSRM/drive system and the baseline motor/drive system, (a) low dP operation and (b) high dP operation.

A histogram of pumping system efficiency for the HRSRM/drive system and the baseline motor/drive system is shown in Fig. 28 for low dP operation. In this mode of operation, the HRSRM/drive system exhibited slightly higher system efficiency than the baseline motor/drive system (59.1 vs. 56.1%, respectively). The difference in system efficiency is significant at the 0.05 significance level, according to the two-sample *t*-test for unpaired data with unequal variances. As noted previously, the HRSRM/drive system operated only 10% of the time in low dP mode, whereas the baseline motor/drive system operated approximately 52% of the time in this mode.

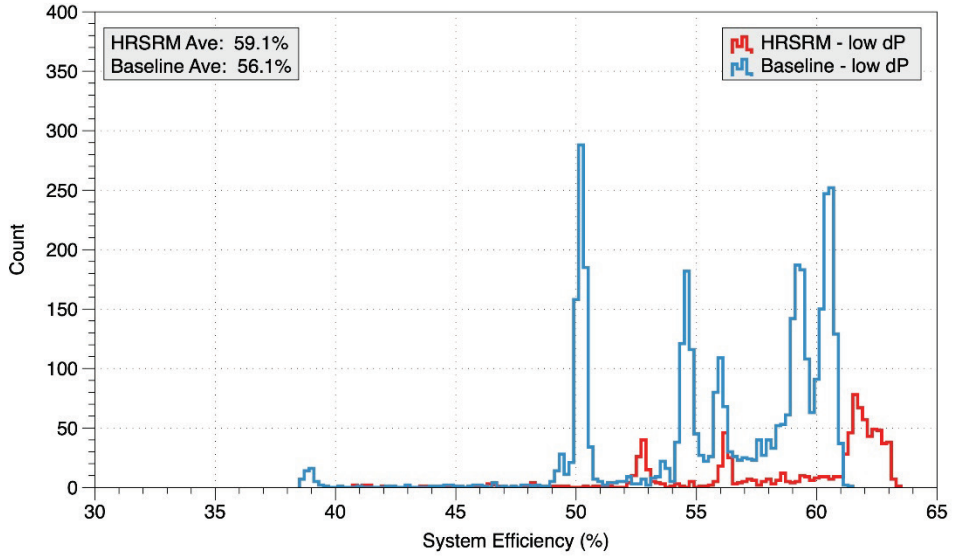

Fig. 28. Histogram of pumping system efficiency for the HRSRM/drive system and the baseline motor/drive system during low dP operation.

A histogram of pumping system efficiency for the HRSRM/drive system and the baseline motor/drive system is shown in Fig. 29 for high dP operation. In this mode of operation, the HRSRM/drive system again exhibited slightly higher system efficiency than the baseline motor/drive system (50.7 vs. 48.9%, respectively). The difference in system efficiency is significant at the 0.05 significance level, according to the two-sample *t*-test for unpaired data with unequal variances. Also, the efficiencies of both the HRSRM/drive system and the baseline motor/drive system were lower in high dP mode than in low dP mode. As noted previously, the HRSRM/drive system operated nearly 90% of the time in high dP mode, whereas the baseline motor/drive system operated approximately 48% of the time in this mode.

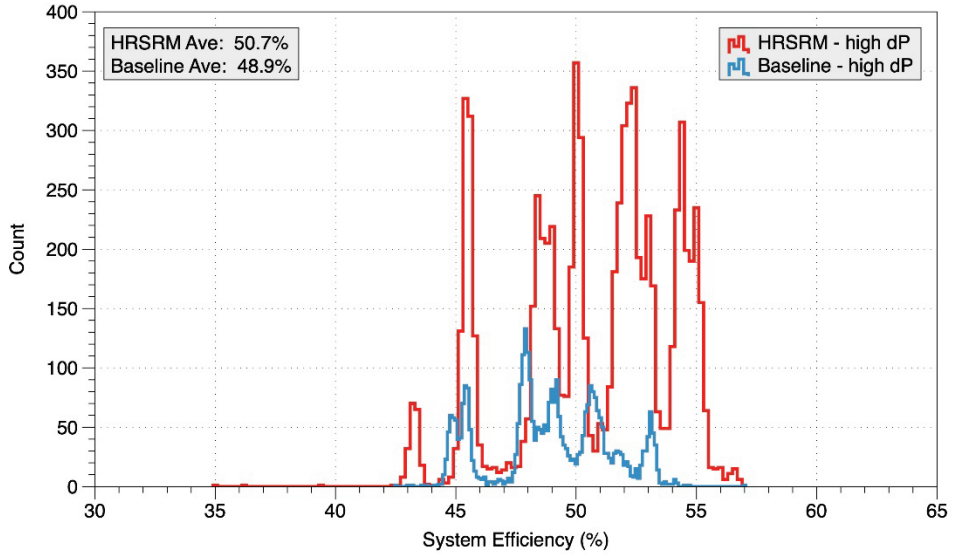

Fig. 29. Histogram of pumping system efficiency for the HRSRM/drive system and the baseline motor/drive system during high dP operation.

A histogram of pumping system efficiency for the HRSRM/drive system and the baseline motor/drive system is shown in Fig. 30 for all modes of operation (low dP and high dP). Since the HRSRM/drive system spent the vast majority of its time operating in the lower-efficiency high dP mode, its overall efficiency was slightly lower than that of the baseline motor/drive system, which operated nearly equally in the higher-efficiency low dP and lower-efficiency high dP modes. Overall, the HRSRM/drive/pump system efficiency was found to be 51.6% and the baseline motor/drive/pump efficiency was found to be 52.7%.

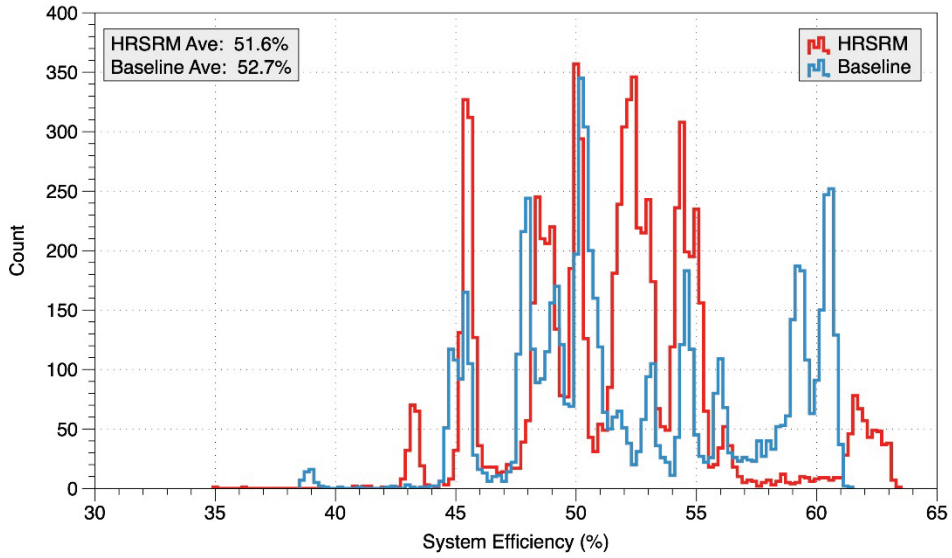

Fig. 30. Histogram of pumping system efficiency for the HRSRM/drive system and the baseline motor/drive system.

A. QUANTITATIVE RESULTS

Laboratory Evaluation Results and Analysis

Based on the results of the laboratory evaluation of the HRSRM, it was found that the HRSRM/drive had on average about 4.5% higher efficiency than a similarly sized premium efficiency induction motor and VFD over a drive frequency range of 20 to 60 Hz.

Field Evaluation Results and Analysis

A summary of the average overall performance of the pumping system with the HRSRM/drive (August 2018) and the baseline motor/drive (September 2018) is shown in Table 4. Also provided in Table 4 is the performance of each motor/drive system during low dP and high dP modes of operation.

Table 4. Summary of pumping system field performance

Performance metric	HRSRM motor/drive	Baseline motor/drive	Difference	
			Absolute	Relative
Overall average				
Hydraulic power (hp)	2.42	2.54	–0.12	–4.7%
System input power (kW)	3.43	3.50	–0.07	–2.0%
System efficiency (%)	51.6	52.7	–1.10	–2.1%
Low dP mode average				
Hydraulic power (hp)	3.26	3.02	0.24	7.9%
System input power (kW)	4.04	3.93	0.11	2.8%
System efficiency (%)	59.1	56.1	3.00	5.3%
High dP mode average				
Hydraulic power (hp)	2.33	2.10	0.23	11.0%
System input power (kW)	3.36	3.04	0.32	10.5%
System efficiency (%)	50.7	48.9	1.80	3.7%

During the field evaluation of the HRSRM, it was found that *for a given operating condition*, the pumping system efficiency was about 3.7 to 5.3% higher with the HRSRM/drive than with the baseline induction motor/drive. Overall, however, pumping system efficiency was slightly lower with the HRSRM/drive than with the baseline motor/drive system (–2.1%), since the HRSRM /drive system spent the vast majority of its time operating in the lower-efficiency high dP mode.

Annual Energy Savings Estimate

The reason for the two modes of operation (I., low dP and high dP) cannot be fully explained. The low dP operating mode was found to occurs generally during nighttime operation, and this mode was characterized by higher motor speeds and higher pumping system efficiencies. Since the two motors did not operate in the two modes for equal amounts of time, an analysis was performed to estimate annual energy consumption, comparing the two motors on an equal basis using the field-measured performance data. To estimate the annual energy savings associated with implementation of the HRSRM/drive as a drop-in replacement for existing motors and drives in this pumping application, the pumping system behavior exhibited by the baseline motor/drive system was used as the basis for comparison. Table 5 shows the operating behavior of the pumping system

with the baseline motor/drive for September 2018, which includes the average delivered hydraulic power for each operating mode (low dP and high dP) and the percentage of time spent in each operating mode. To estimate the annual energy consumption of the two motor/drive systems, this behavior was assumed to persist throughout the entire year.

Table 5. Pumping system behavior for annual energy estimation

Operating mode	Average delivered hydraulic power (hp)	Time in operating mode (%)
Low dP	3.02	52
High dP	2.10	48

The average system input power for each motor, $\dot{W}_{in}$, is then determined as follows:

$$\dot{W}_{in} = t_{low}\left(\frac{\dot{W}_{hydr,low}}{\eta_{low}}\right) + t_{high}\left(\frac{\dot{W}_{hydr,high}}{\eta_{high}}\right),$$

where t_{low} is the fraction of time spent in the low dP operating mode, $\dot{W}_{hydr,low}$ is the average delivered hydraulic power in the low dP mode, η_{low} is the average system efficiency for the low dP mode, t_{high} is the fraction of time spent in the high dP operating mode, $\dot{W}_{hydr,high}$ is the average delivered hydraulic power in the high dP mode, and η_{high} is the average system efficiency for the high dP mode.

For the baseline motor/drive system, the average system input power is estimated to be

$$\dot{W}_{in,baseline} = (0.52)\left[\frac{3.02\text{ hp}}{0.561}\right] + (0.48)\left[\frac{2.10\text{ hp}}{0.489}\right] = 4.86\text{ hp} = 3.62\text{ kW}.$$

For the HRSRM /drive system, the average system input power is estimated to be

$$\dot{W}_{in,HRSRM} = (0.52)\left[\frac{3.02\text{ hp}}{0.591}\right] + (0.48)\left[\frac{2.10\text{ hp}}{0.507}\right] = 4.65\text{ hp} = 3.47\text{ kW}.$$

Noting that there are 8,760 hours per year, and assuming continuous operation, the estimated annual energy consumption of the two pump motor/drive systems becomes

- Baseline: 31,700 kWh
- HRSRM: 30,400 kWh

The annual energy savings associated with the HRSRM/drive for this pumping application, compared with the baseline induction motor and drive, is estimated to be 1,300 kWh, or 4%. In addition, assuming an average cost of electricity for commercial customers in California of \$0.1759/kWh[4], the annual energy cost savings for the HRSRM retrofit is estimated to be approximately \$230.

[4] EIA. 2018. Electric Power Monthly with Data for September 2018. U.S. Energy Information Administration, U.S. Department of Energy, Washington, D.C.

B. QUALITATIVE RESULTS

Ease of Installation and Deployment

The manufacturer of the HRSRM /drive claims that its system is a drop-in replacement for existing motors and drives. The 10 hp HRSRM used in this study was manufactured to comply with standard NEMA frame sizes and dimensions, resulting in common dimensions for shaft diameter, shaft height, shaft length, and bolt hole spacing and location. Specifically, the 10 hp HRSRM was manufactured to comply with the NEMA 215T frame size.

According to staff at the San Ysidro facility, the process of installing the HRSRM was no different from that required for any other motor. Since the HRSRM complies with the NEMA 215T frame size, the HRSRM was easily bolted directly to the existing pump assembly, and the motor shaft was easily coupled to the pump shaft. During installation, San Ysidro facilities staff made use of a laser shaft alignment tool to ensure that the HRSRM shaft was properly aligned to the pump shaft.

The electrical connections at the HRSRM are made through a junction box mounted directly on the motor casing. This junction box was supplied by the manufacturer with one knock-out through which the electrical wiring (presumably both power and controls) were intended to pass. The San Ysidro facility staff drilled an additional hole in the motor's electrical junction box to allow power wiring and controls wiring to enter through separate holes in the junction box. It is the recommendation of the San Ysidro facilities staff that the junction box on the HRSRM be provided with two knock-outs, one for power wiring and the other for controls wiring. It is also suggested that these knock-outs should accept ¾ inch electrical conduit and fittings.

The San Ysidro facilities staff connected the power and controls wiring to the HRSRM before the arrival of the manufacturer and ORNL staff. In addition, power wiring was installed to the HRSRM controller. Upon the arrival of the manufacturer and ORNL staff, it was noted that the power wiring was installed correctly. The San Ysidro staff noted an inconsistency in the color coding of the controls wiring, which led to some confusion about the proper wiring of the controls at the motor. Since no instructions were provided to the San Ysidro facilities staff regarding how to wire the controls signals at the HRSRM controller, the controls signal wiring was not completed by the San Ysidro staff before the manufacturer's and ORNL staff arrived. After the manufacturer and ORNL staff arrived, the San Ysidro facilities staff successfully wired the controls signals to the HRSRM and controller, with the guidance of the manufacturer's staff.

Installation and Commissioning

The San Ysidro facility building automation system (BAS) provides a pump motor speed control signal that varies from 2.5 to 10 V. This voltage range corresponds to a pump motor rotational speed of 440 to 1760 RPM. SMC staff programmed the HRSRM controller on-site so that the HRSRM rotational speed would range from 440 to 1760 RPM in proportion to the BAS control signal of 2.5 to 10 V. For a control signal of less than 2.5 V, the motor controller was programmed to provide a rotational speed of 440 RPM.

The programming of the HRSRM controller is performed by directly connecting a computer to the motor controller and using a proprietary software application to access and set the motor controller parameters.

The ability to control motor speed properly was verified by directly setting the speed within the BAS and noting that the actual motor speed, as indicated by a computer connected to the HRSRM controller, matched that set in the BAS.

Operations and Maintenance

Upon successful wiring of the power and controls for the HRSRM and controller, the HRSRM was started via the facility's BAS. Immediately upon starting, and subsequently during its operation, it was noted that the HRSRM was significantly louder than the original pump motor (Baldor EM3774T).

In addition, after the HRSRM startup, San Ysidro facilities staff wanted feedback from the motor controller regarding various motor parameters, such as current draw, power consumption, and rotational speed. This information is not directly available from the HRSRM controller, as opposed to the original pump motor controller that has an LCD display that can provide various operational parameters. Note, however, that HRSRM parameters can be viewed via a computer attached to the HRSRM controller.

The bearings of the HRSRM are permanently sealed, and, thus, no regular lubrication or maintenance is required for the HRSRM.

Occupant Satisfaction

During the period for which the HRSRM/drive was operational in the chiller pump application; there were no reports of occupant dissatisfaction with the internal environment (*i.e.*, temperature, and humidity) of the building spaces served by the chiller.

However, from the perspective of the San Ysidro facilities staff, there was dissatisfaction with the noise produced by the HRSRM/drive. Facilities staff expressed concern that hearing protection would be required when performing work for extended periods of time near the HRSRM/drive.

Sound level measurements were made during the laboratory evaluation of the HRSRM/drive and, on average, the sound level of the HRSRM was 94 dBA, while the sound level of the baseline induction motor was 79 dBA. Details of the sound level measurements performed by North Carolina Advanced Energy Corporation may be found in Appendix B.

C. COST-EFFECTIVENESS

For an existing induction motor/drive, the HRSRM/drive can be either an energy efficiency retrofit or an end-of-life equipment replacement. The cost effectiveness of the HRSRM/drive is estimated for either a retrofit or an end-of-life replacement, and the energy savings and payback for either scenario are summarized in Table 6 and Table 7, respectively. In the cost effectiveness analyses, the baseline or current industry standard replacement was assumed to consist of a NEMA premium efficiency motor with a VFD, and pricing for the current industry standard equipment was provided by San Ysidro LPOE engineering personnel. Pricing for the tested technology represents a best-case scenario for volume pricing of the HRSRM/drive as provided by the manufacturer. Annual energy costs were estimated using average California utility rate data.

In an energy efficiency retrofit scenario, the HRSRM/drive system results in a simple payback period of 14.8 years. On the other hand, for an end-of-life equipment replacement scenario, the

HRSRM/drive system results in an immediate simple payback, since this new technology is less expensive than the industry-standard replacement and the new technology provides a slight energy cost savings.

Table 6. Economic assessment (retrofit scenario)

	Baseline (Before)	Tested technology (After)	Difference
Equipment cost[1]	N/A	$2,430	N/A
Installation cost[2]	N/A	$948	N/A
Total cost per unit	N/A	$3,378/unit	N/A
Annual maintenance cost	$0/year	$0/year	$0/year
Annual energy consumption	31,700 kWh/year	30,400 kWh/year	1,300 kWh/year
Annual energy cost (@ $0.1759/kWh)[3]	$5,576/year	$5,347/year	$229/year
Simple payback		14.8 years	
Savings-to-investment ratio[4]		0.81	

[1]Tested technology costs provided by the HRSRM/drive manufacturer and do not include volume discounts.
[2]Labor cost estimate provided by San Ysidro LPOE engineering personnel: 12 hours @ $79/hr GSA contract rate. Pump applications require laser alignment to align pump and motor shafts.
[3]Energy costs based on average California utility rates.
[4]Equipment lifespan is 12 years.

Table 7. Economic assessment (end-of-life scenario)

	Industry-standard replacement	Tested technology (After)	Difference
Equipment cost[1]	$4,375	$2,430	$1,945
Installation cost[2]	$948	$948	$0
Total cost per unit	$5,323/unit	$3,378/unit	$1,945/unit
Annual maintenance cost	$0/year	$0/year	$0/year
Annual energy consumption	31,700 kWh/year	30,400 kWh/year	1,300 kWh/year
Annual energy cost (@ $0.1759/kWh)[3]	$5,576/year	$5,347/year	$229/year
Simple payback		Immediate	
Savings-to-investment ratio[4]		1.41	

[1]Industry standard replacement costs provided by San Ysidro LPOE engineering personnel. Tested technology costs provided by the HRSRM/drive manufacturer and do not include volume discounts.
[2]Labor cost estimate provided by San Ysidro LPOE engineering personnel: 12 hours @ $79/hr GSA contract rate. Pump applications require laser alignment to align pump and motor shafts.
[3]Energy costs based on average California utility rates.
[4]Equipment lifespan is 12 years.

IV. Summary Findings and Conclusions

A. OVERALL TECHNOLOGY ASSESSMENT AT DEMONSTRATION FACILITY

The laboratory performance evaluation of the HRSRM/drive revealed that on average, this technology is 4.5% more efficient than a premium efficiency induction motor and VFD. During the laboratory performance evaluation, it was found that the HRSRM did show somewhat inconsistent performance at the two lowest speeds tested. The manufacturer has independently acknowledged this issue, which was related to the system under test being an early production system. The manufacturer has since improved the software control algorithms, and that modification has completely mitigated the low-speed motor performance issue identified during the laboratory testing.

During the field demonstration, it was noted that, for a given operating condition, the HRSRM/drive provided 3.7 to 5.3% higher pumping system efficiency than the baseline induction motor/drive. However, over the duration of the field demonstration, it was found that the pumping system coupled with the HRSRM/drive operated at a lower efficiency than when it was operating with the baseline motor/drive.

For the pumping application investigated in this demonstration, the estimated annual energy savings of the HRSRM/drive retrofit was 1,300 kWh, or 4%. Assuming an average cost of electricity for commercial customers in California of $0.1759/kWh, the annual energy cost savings for the HRSRM/drive retrofit is estimated to be $230.

The HRSRM motor/drive system is software-enabled and includes built-in sensors to measure speed, torque, and temperature. Operating data from these sensors can be transmitted to the manufacturer's cloud-based storage system, thereby allowing remote monitoring of motor performance. Alerts can be sent to operators when motor performance degrades or when faults are detected. In addition, operating parameters can be updated remotely through the cloud connection. Note that implementation of these cloud-based capabilities in GSA facilities requires cybersecurity assessment, authorization, and continuous monitoring. Given the considerable effort and time associated with GSA's cybersecurity screening process, it was decided at the beginning of this project to forgo this screening process and not utilize or evaluate the cloud-based features of the HRSRM/drive.

B. LESSONS LEARNED AND BEST PRACTICES

The process of installing the HRSRM was no different from that required for any other motor. Since the HRSRM complies with the NEMA 215T frame size, the HRSRM was easily bolted directly to the existing pump assembly and the motor shaft was easily coupled to the pump shaft.

While the electrical connections were being made to the HRSRM, it was noted that the junction box on the motor had only one knock-out through which the electrical wiring (presumably both power and controls) were intended to pass. The San Ysidro facility staff drilled an additional hole in the motor's electrical junction box to allow power wiring and controls wiring to enter through separate

holes in the junction box. It is recommended that the junction box on the HRSRM be provided with two knock-outs, one for power wiring and the other for controls wiring. It is also suggested that these knock-outs should accept ¾ inch electrical conduit and fittings.

Immediately upon starting and subsequently during its operation, it was noted that the HRSRM was significantly louder than the original pump motor. Facilities staff expressed concern that hearing protection would be required for performing work for extended periods of time near the HRSRM/drive. The manufacturer recognized the noise issue for the HRSRM and has been actively engaged in improving the design of the motor to reduce the noise. While the manufacturer claims to have a new motor design which reduces the noise, the degree to which the noise level has been reduced has not yet been independently verified via a third party.

In addition, after the HRSRM startup, San Ysidro facilities staff wanted feedback from the motor controller regarding various motor parameters, such as current draw, power consumption, and rotational speed. This information is not directly available from the HRSRM controller, as opposed to the original pump motor controller, which has an LCD display that can provide various operational parameters. Note however, that HRSRM motor parameters can be viewed via a computer attached to the HRSRM controller.

C. DEPLOYMENT RECOMMENDATIONS

For the pumping application investigated in this motor demonstration, it was found that a small energy benefit could be realized by retrofitting the existing NEMA premium efficiency induction motor and VFD with the manufacturer's HRSRM/drive system. In addition, the manufacturer's motor controller can conveniently provide useful information related to motor performance during operation, which may be beneficial for fault diagnostic purposes.

Note that the HRSRM/drive technology has also been evaluated by the National Renewable Energy Laboratory (NREL) for a different application—condenser fans used in commercial refrigeration systems.[5] A demonstration at a Walmart Supercenter (#5957) in Lakeside, Colorado, was performed. The commercial refrigeration system at the site consists of two compressor racks, each with medium- and low-temperature loads. One compressor rack is connected to a condenser with ten 1.5 hp condenser fan motors controlled by one VFD, and the other compressor rack is connected to a condenser with eight 1.5 hp condenser fan motors controlled by a separate VFD. The 1.5 hp legacy induction motors driving the condenser fans have nameplate efficiencies of 73.5%. Nine HRSRMs replaced nine of the legacy induction motors. According to the manufacturer, its HRSRM can achieve up to 95% peak motor efficiency and maintain similarly high levels of performance over a wide range of operating speeds and torques.

Based on measured data from the test site, a power savings curve for the condenser fan motors was generated to estimate the power savings of the HRSRM as a function of motor speed, as shown in Fig. 31. It can be seen from the NREL study that energy savings for the HRSRM increase with

[5] Wheeler, Grant, and Deru, Michael. 2018. Direct Comparison of High Rotor Pole Switched Reluctance Motors as Condenser Fans in a Commercial Refrigeration System. NREL/TP-5500-72476, National Renewable Energy Laboratory (NREL), Golden, Colorado.

decreasing motor speed. Also, energy savings of at least 30% were achieved by replacing the legacy condenser fan motors with HRSRMs.

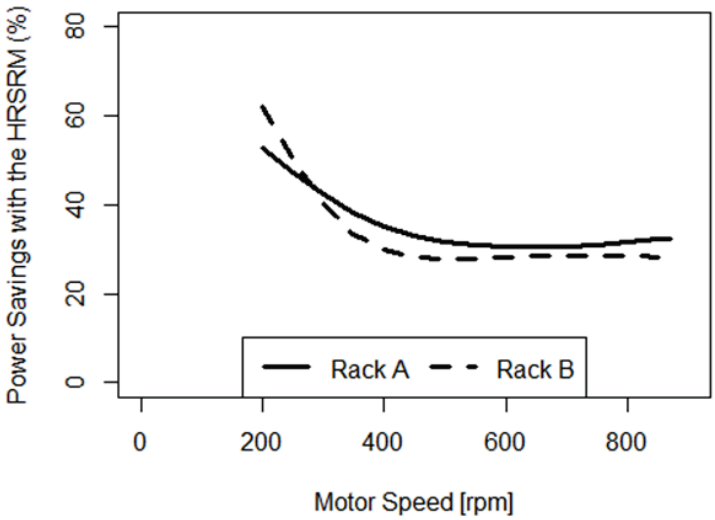

Fig. 31. Power savings with the HRSRM, based on an NREL study of commercial refrigeration condenser fan motors[5].

In addition, in the NREL study, energy savings were estimated for three different condenser fan operating scenarios. These three scenarios include:

- Replacing a constant-speed induction motor with a constant-speed HRSRM;
- Replacing a variable-speed induction motor with a variable-speed HRSRM; and
- Replacing a constant-speed induction motor with a variable-speed HRSRM.

As shown in Table 8, the condenser fan energy savings for these three scenarios ranged from 29 to 71%. The greatest energy savings occurred as a result of replacing a constant-speed induction motor with the variable-speed HRSRM.

Table 8. Estimated energy savings for various condenser fan motor retrofit scenarios[5]

Scenario	Baseline control	Baseline motor	Retrofit control	Retrofit motor	Energy savings
1	Constant fan speed	Induction	Constant fan speed	HRSRM	29%
2	Variable fan speed	Induction	Variable fan speed	HRSRM	33%
3	Constant fan speed	Induction	Variable fan speed	HRSRM	71%

Compared with the present study, a much greater relative energy savings was noted in the NREL study. However, the legacy motors that were replaced in the NREL study were significantly lower in efficiency than the HRSRM used in the San Ysidro LPOE retrofit. Furthermore, in this demonstration, the HRSRM replaced a NEMA premium efficiency motor. Since lower-power induction motors generally have lower efficiencies than higher-power induction motors (see Fig. 5), greater relative energy savings will result from retrofitting lower-power induction motors with HRSRMs.

Based on both this demonstration and the NREL demonstration, it is recommended that for end-of-life replacement and for new construction, fixed-speed induction motors be replaced with the manufacturer's HRSRM/drive system. Also, it is recommended to retrofit lower-power induction motors/drives (less than 5 hp) with the HRSRM/drive, since, as noted above, greater relative energy savings will result from retrofitting lower-power induction motors with HRSRMs. Finally, for larger motors (5 hp or greater), the HRSRM can be an energy-efficient end-of-life equipment replacement solution for legacy NEMA premium efficiency motors.

Finally, note that the Buy American Act of 1933 (Title 41 U.S. Code §§ 8301-8305) requires that every contract for the construction, alteration or repair of any public building in the United States shall use only articles that have been manufactured in the United States. Since the HRSRM/drive evaluated in this study is manufactured in China, it does not sufficiently support the Buy American Act of 1933. A waiver of the Buy American Act will be required to implement the HRSRM/drive system in GSA facilities.

V. Appendices

Appendix A: ABBREVIATIONS AND ACRONYMS

The following is a list of abbreviations, acronyms, and terms used in this report.

Term	Description
A	ampere
BAS	building automation system
CT	current transformer
dBA	decibel, A-weighted
DOE	U.S. Department of Energy
dP	pressure differential
EPAct	Energy Policy Act
ft	foot, feet
GPG	GSA Proving Ground Program
GPM	gallons per minute
GSA	U.S. General Services Administration
HIT	High Impact Technology Catalyst Program
hp	horsepower
HRSRM	high rotor pole switched reluctance motor
HVAC	Heating, ventilation and air-conditioning
Hz	hertz
kW	kilowatt
kWh	kilowatt hour
lb	pound force
lb_m	pound mass
LCD	liquid crystal display
LPOE	land port of entry
m	meter
N	newton
NEMA	National Electrical Manufacturers Association
NREL	National Renewable Energy Laboratory
O&M	operations and maintenance
ORNL	Oak Ridge National Laboratory

Term	Description
psig	pounds per square inch gauge
RPM	revolutions per minute
SMC	Software Motor Company
SR	switched reluctance
SRM	switched reluctance motor
V	volt
VFD	variable frequency drive
W	watt

Appendix B: LABORATORY TESTING

REPORT

Oak Ridge National Lab Comparative Electric Motor Testing

December 17th, 2018

Authored By:
Advanced Energy

Introduction

Dr. Brian A. Fricke of Oak Ridge National Laboratory (ORNL) approached Advanced Energy in May 2017 looking to perform comparative electric motor testing. The testing is related to a demonstration that Dr. Fricke is working on that deals with a switched reluctance (SR) motor design. The motor is designed by Software Motor Corporation (SMC) of Sunnyvale, CA. ORNL has previously completed field testing on this product. The laboratory testing is to evaluate the performance of the SR motor versus a commercially available premium efficiency induction machine. The SMC motor, SMC VFD and Baldor motor were supplied by ORNL. An appropriately sized Yaskawa VFD was supplied by Advanced Energy to be used as a means to vary the speed of the Baldor motor. This report presents the findings of that comparison.

Test Procedure

Test Setup

Each motor was mounted and aligned to Advanced Energy's AC Dynamometer as shown below in Figures 1 and 3. A Yokogawa WT3000 Precision Power Analyzer recorded the input electrical measurements into each VFD. A torque transducer was used to record the output mechanical measurements at the motor shaft. The SMC motor setup is shown in Figure 1 and the SMC VFD is shown in Figure 2. The Baldor motor setup is shown in Figure 3 and the Yaskawa VFD is shown in Figure 4. A complete schematic of the test setup is shown in Figure 5.

Figure 1: SMC motor on dynamometer

Figure 2: SMC VFD

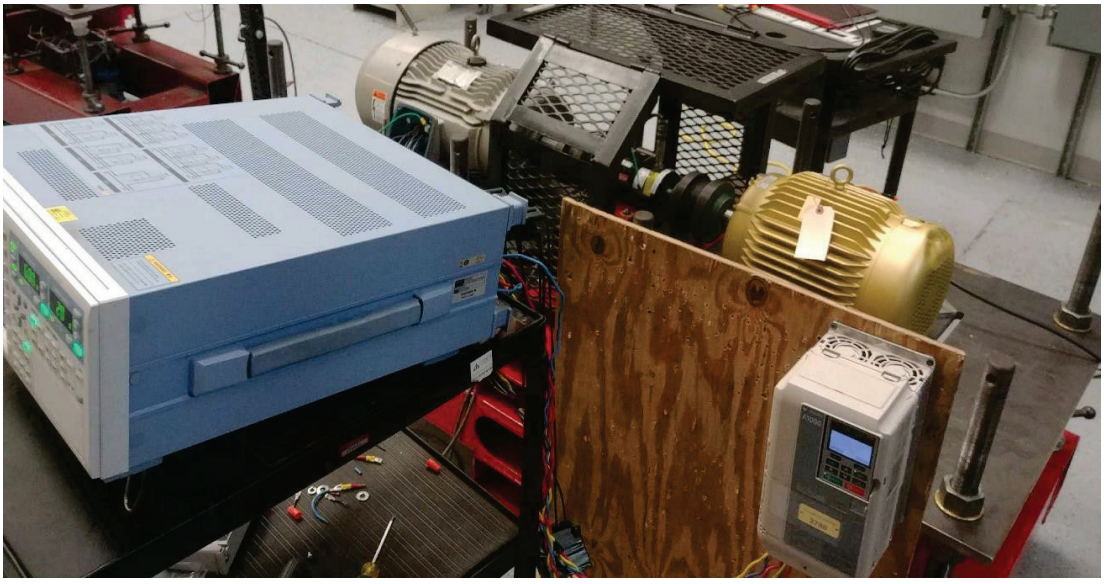

Figure 3: Baldor motor on dynamometer

Figure 4: Yaskawa VFD

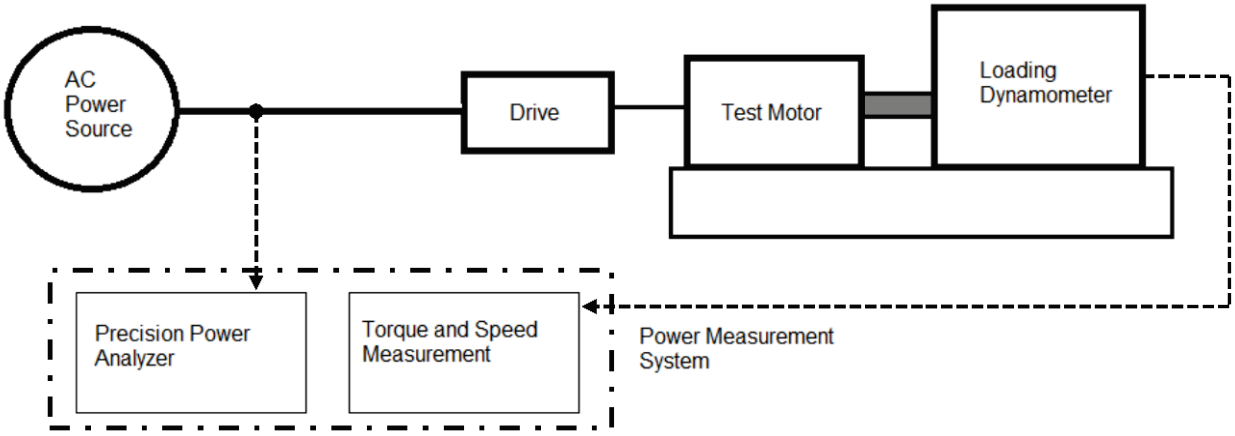

Figure 5: Schematic of the test setup

VFD Setup

The SMC motor and VFD combination was supplied with its own control software. The control software was downloaded to an Advanced Energy computer and used to control the speed setting of the SMC motor during testing. The SMC VFD was already programmed before arrival at the Advanced Energy lab. No changes were made to the SMC VFD parameters prior to testing.

The Baldor motor and Yaskawa VFD combination was controlled via keypad on the Yaskawa VFD itself. At the request of ORNL the Yaskawa VFD was operated in Volts/Hertz mode and default parameters were maintained. The only parameters changed from defaults for this testing were motor nameplate parameters specific to the Baldor motor shown in Appendix A. No auto tuning was performed and no attempt was made to determine the most efficient control method of the Baldor motor and Yaskawa VFD combination.

Test Data Points

Each motor was tested over the range of speeds and torques indicated in Table 1. The torque set points in Table 1 were calculated as a percentage of rated full load torque of the Baldor motor and the same values were used for testing of the SMC motor. Prior to taking data points, each motor was thermally stabilized. Advanced Energy's stabilization criterion requires the temperature rise of the motor to change by less than 1°C over a 30 minute period. After this criterion was met, the motor was operated at varying torque loads and speed points while data was collected.

For both motors, the machine was operated at a setting of 60.0Hz on the respective VFD with a target torque of approximately 40Nm until the motor was thermally stable for each case. This was rated full load torque of the motor based on nameplate data (see Appendix A). For the temperature measurement, the Baldor motor was opened and a thermocouple placed directly on the windings. The drive end endbell was then replaced in the same manner as it had been removed. For the other machine, it was advised by ORNL not to open the SMC motor. Due to that request, the thermocouple was placed on the motor casing at position 12 o'clock on the drive end.

TORQUE	Frequency (Hz)								
(%)	60.0	53.3	46.7	40.0	33.3	26.7	20.0	13.3	6.7
100	X	X	X	X	X	X	X	X	X
90	X	X	X	X	X	X	X	X	X
80	X	X	X	X	X	X	X	X	X
70	X	X	X	X	X	X	X	X	X
60	X	X	X	X	X	X	X	X	X
50	X	X	X	X	X	X	X	X	X
40	X	X	X	X	X	X	X	X	X
30	X	X	X	X	X	X	X	X	X
20	X	X	X	X	X	X	X	X	X
10	X	X	X	X	X	X	X	X	X

Table 1: Test Data Points

Test Results

A performance comparison was carried out on the basis of system efficiency. The system efficiency is calculated as a ratio of shaft output power to electrical input power into the VFD. Plots of system efficiency are presented in Figures 6 – 14. Raw data for both motor tests is supplied in a separate file titled “ORNL Raw Data.xlsx”.

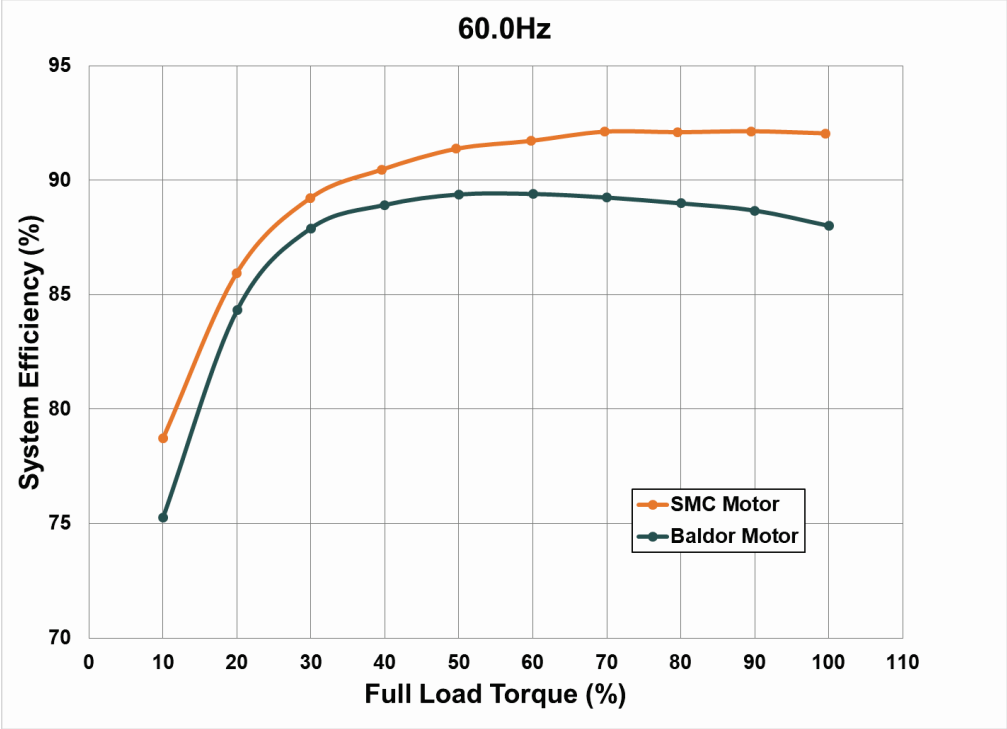

Figure 6: System efficiency comparison at 60.0Hz

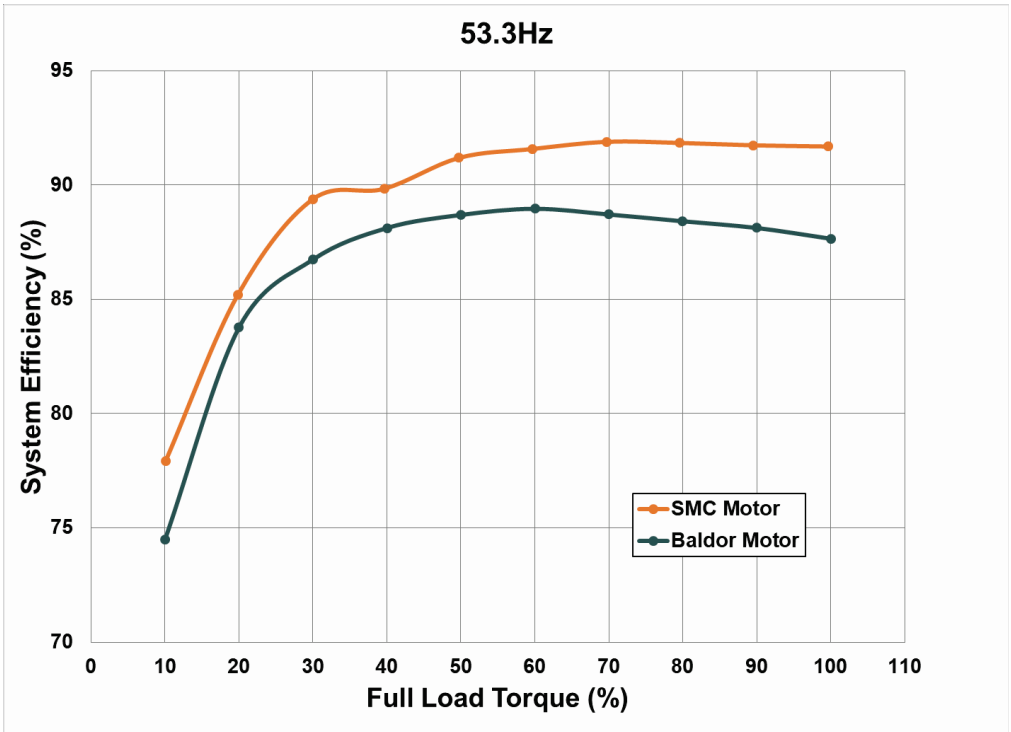

Figure 7: System efficiency comparison at 53.3Hz

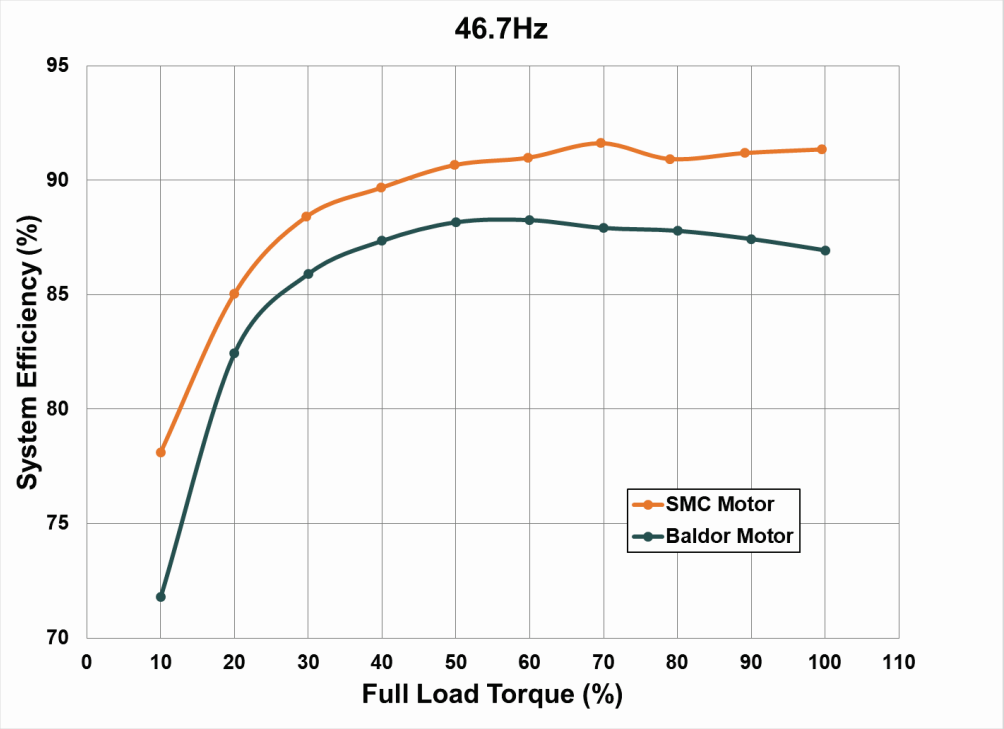

Figure 8: System efficiency comparison at 46.7Hz

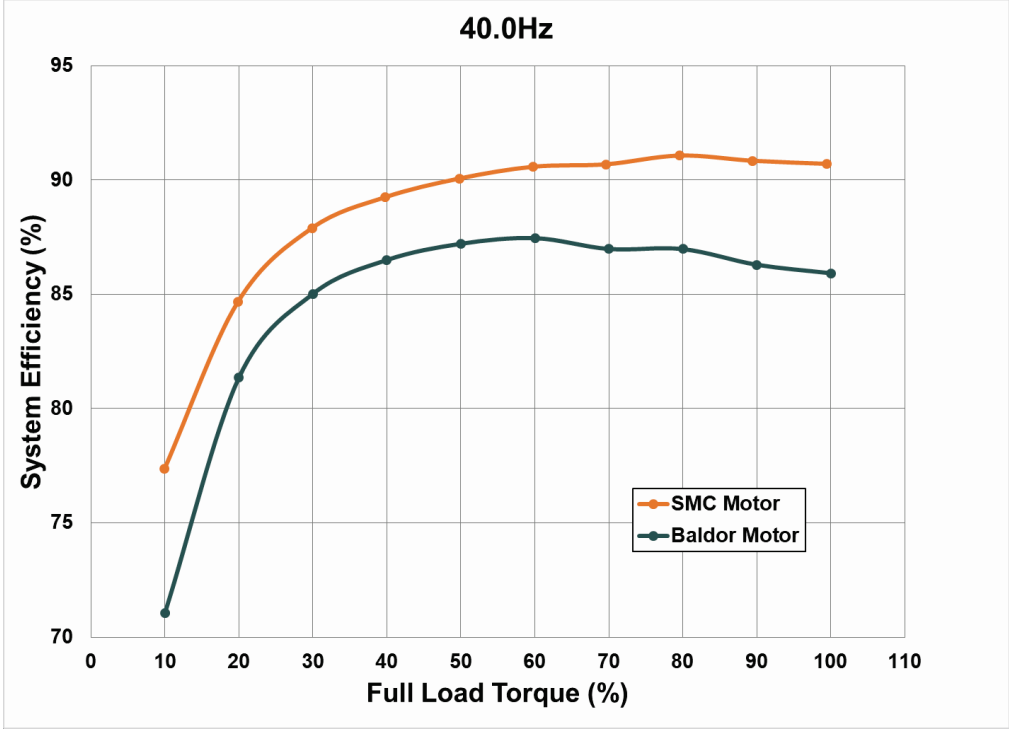

Figure 9: System efficiency comparison at 40.0Hz

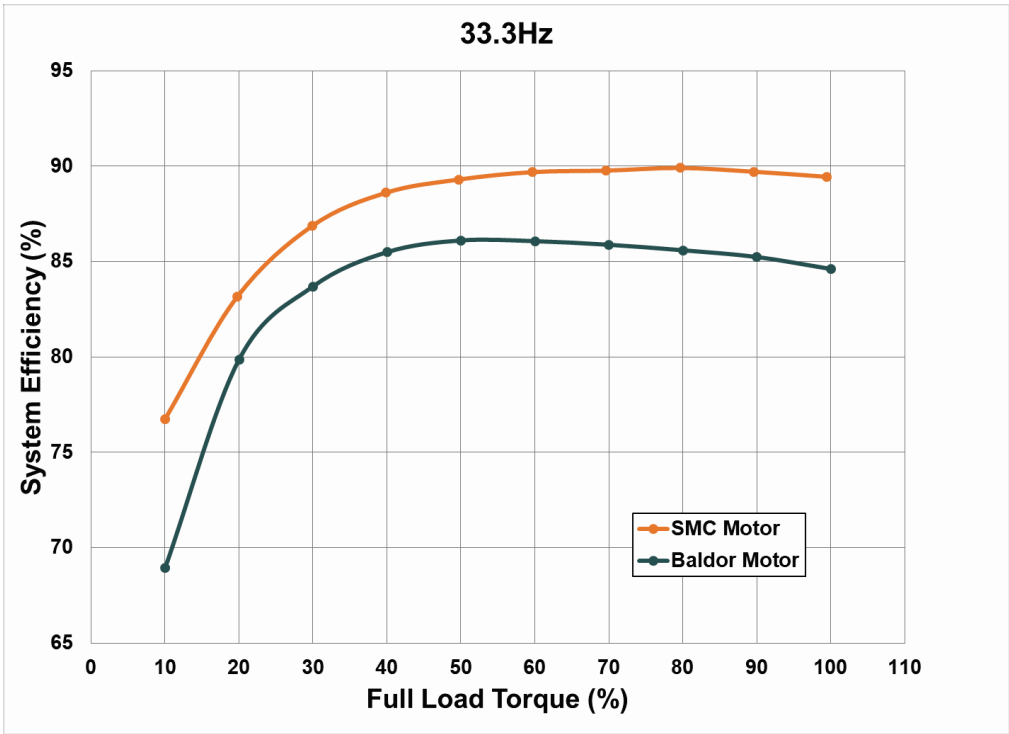

Figure 10: System efficiency comparison at 33.3Hz

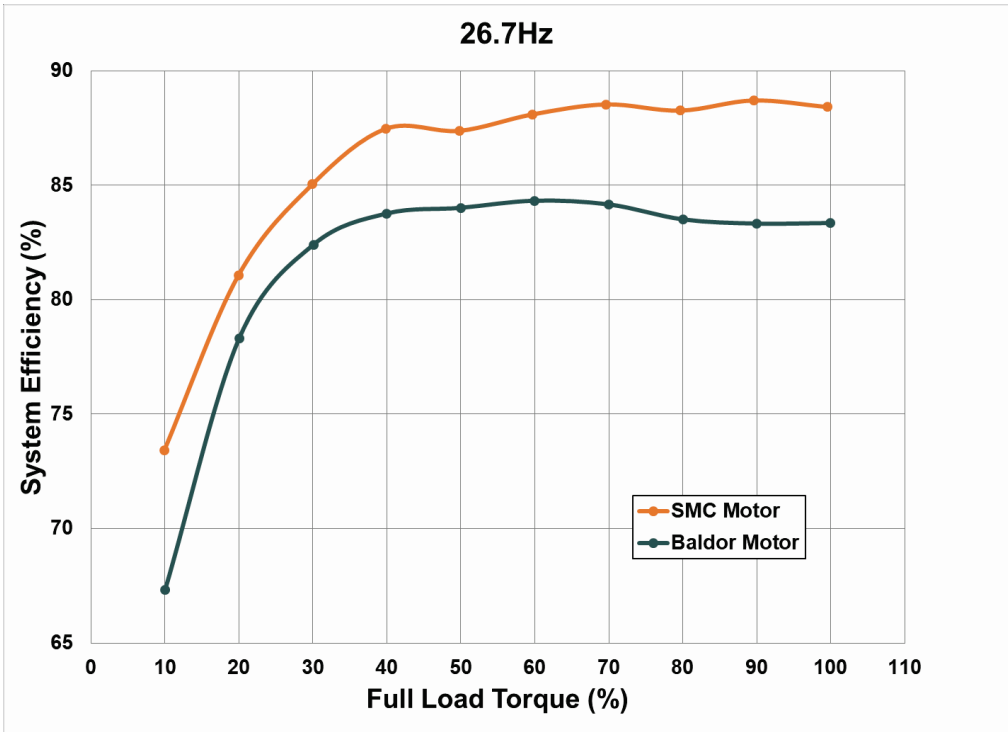

Figure 11: System efficiency comparison at 26.7Hz

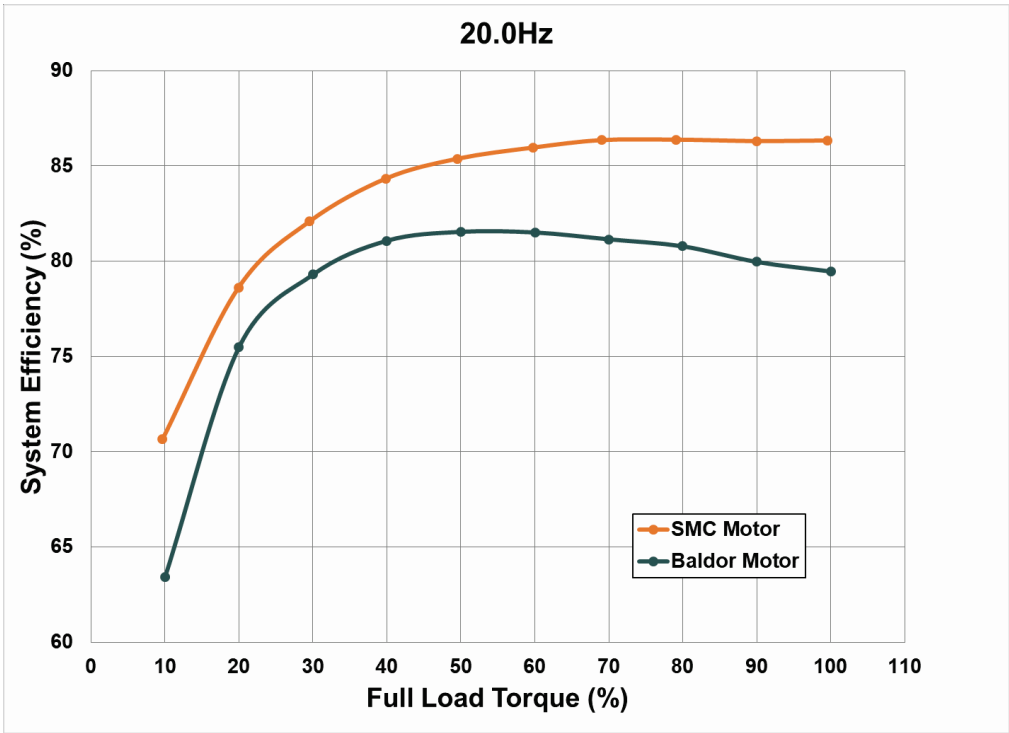

Figure 12: System efficiency comparison at 20.0Hz

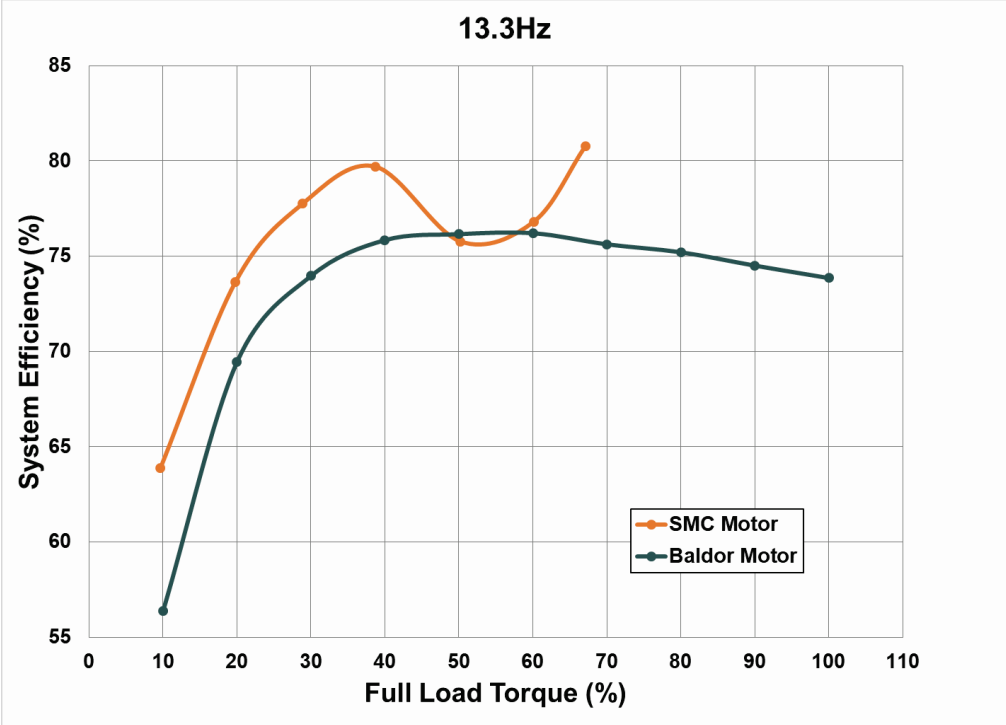

Figure 13: System efficiency comparison at 13.3Hz

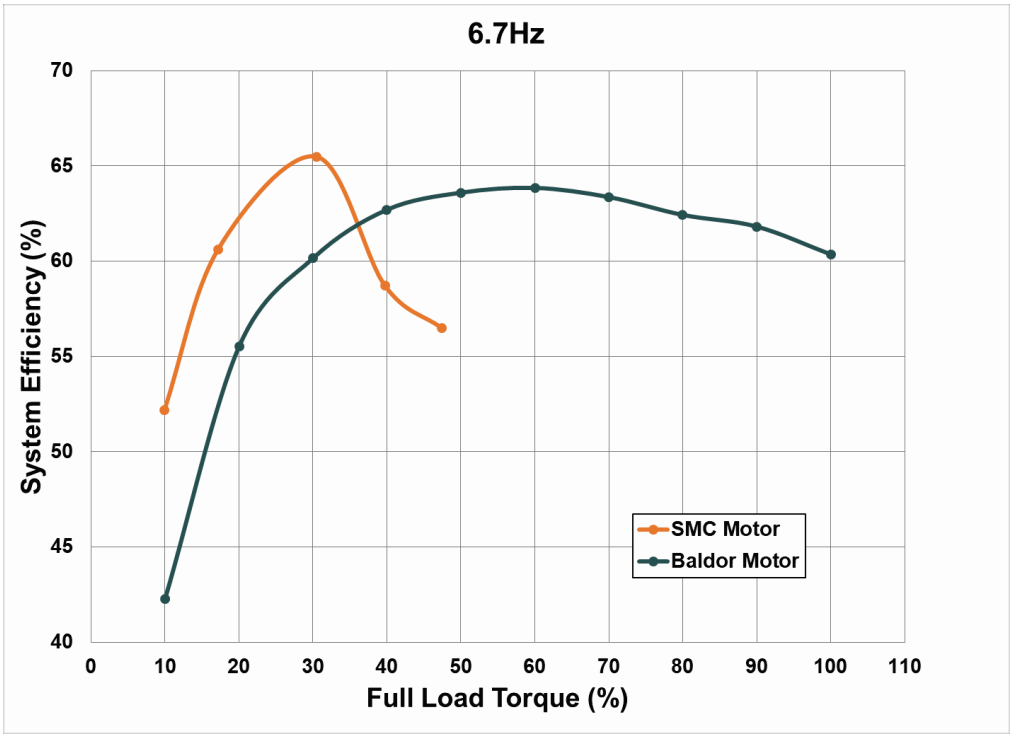

Figure 14: System efficiency comparison at 6.7Hz

Conclusion

Comparative testing of a 10Hp switched reluctance motor manufactured by SMC and a 10Hp commercially available induction motor (Baldor) was carried out. Both motors were operated with variable frequency drives and ran at many different test speeds with the objective of comparing system efficiency. The SMC motor and VFD combination was supplied with its own software. Advanced Energy staff simply input a target speed into the supplied program and the motor would spin at that speed. The Baldor motor was operated by an off the shelf Yaskawa VFD. The Baldor induction motor tested was was supplied by Oak Ridge National Lab for the purpose of this test. The Yaskawa VFD was supplied by the Advanced Energy lab and was the closest VFD in output rating to the Baldor motor that Advanced Energy has in inventory. The Baldor and Yaskawa combination was operated in Volts/Hertz mode via the keypad and no attempt was made to find the most efficient control method.

From the test results, the system efficiency of the SMC motor was consistently higher than the induction motor at nearly all tested speed and load points for each comparison set. The SMC motor did show some inconsistent performance at the two lowest speeds that was not observed with the Baldor motor. The SMC motor was unable to achieve full load torque at the two lowest speeds and the data recorded was unstable. It is not known if this inconsistency stems from the motor itself or the control algorithm.

Appendix A: Nameplate Information of Motors and VFDs.

Motor Nameplate Data		
	SMC Motor	Baldor Motor
Model Number	V03-1000-4-D00	EM3774T
Output Rating	10.0Hp	10.0Hp
Voltage (V)	680Vdc	208-230/460
Current (A)	21.5	26.5-24.4/12.2
Speed (RPM)	1800	1760
Frequency (Hz)	-	60
Service Factor	1.15	1.15
Frame	213T/215T	215T
Enclosure	TEFC	TEFC
Insulation Class	F	F
Duty	Continuous	Continuous
Efficiency	94.0%	91.7%

VFD Nameplate Data		
	SMC VFD	Yaskawa VFD
Model Number	SMC-P05-EX	CIMR-AU4A0018FAA
Input Voltage (V)	460	380-480
Input Current (A)	1.8-16	20/15
Input Freq. (Hz)	60	60
Output Voltage (V)	280dc-680dc	0-480
Output Current (A)	-	17.5/14.8
Output Freq. (Hz)	-	0-400

Appendix C: SOUND LEVEL MEASUREMENTS

SOUND LEVEL MEASUREMENTS

Sound Test per MG-1-Part 9 - 2016

Instrument Used:
Rion Sound Level Meter NA-24 S/No. 11273483
Rion UC-52 Microphone S/No. 58120

Sound Results (Full Load)

Test Motor	Sound (dB)				
	2X	1Y	2Y	1X	1Z
Baldor Motor	N/A	78.0	N/A	80.0	79.7
SMC Motor	N/A	96.2	N/A	92.5	92.2

*All readings taken 1m away from center of motor